Chinese Chemical Letters 32 (2021) 2679–2692

Contents lists available at ScienceDirect

Chinese Chemical Letters

journal homepage: www.elsevier.com/locate/cclet

Review

Recent advances in nonmetallic atom-doped metal nanocrystals: Synthesis and catalytic applications

Ruiyun Guo, Ke Zhang, Shangdong Ji, Yangzi Zheng, Mingshang Jin*

Frontier Institute of Science and Technology and State Key Laboratory of Multiphase Flow in Power Engineering, Xi'an Jiaotong University, Xi'an 710049, China

ARTICLE INFO

Article history:
Received 30 December 2020
Received in revised form 2 February 2021
Accepted 3 February 2021
Available online 17 March 2021

Keywords:
Nonmetallic atom-doping
Metal-nonmetal nanocrystals
Organic catalysis
Electrocatalysis
Catalyst design

ABSTRACT

Metal nanocrystals have been recognized as the main catalytic materials in many fields, but insufficient activity and stability, as well as high prices, have limited their large-scale potential applications. As one of the extremely promising alternatives toward metal in boosting their catalytic performance, nonmetallic atoms-doped metal nanocrystals have recently received extensive attention because of their high efficiency, chemical and structural durability, abundant reserve, and low cost. In this review, we highlight the most recent progress in this field and provide insights into their catalytic applications. The metal-nonmetal nanocrystals prepared by doping metal nanocrystals with nonmetallic atoms are introduced and classified based on the types of nonmetallic atoms, including metal hydrides, borides, carbides, nitrides, oxides, phosphides, and chalcogenides. Besides, their applications in catalysis, especially in electrocatalysis and organic catalysis, have been summarized and discussed. Finally, the conclusions and perspectives are given for the catalysis-driven rational design of metal-nonmetal nanocrystals in this minireview.

1. Introduction

As one of the important parts of nanomaterials, metal nanocrystals own intriguing electronic, optical, magnetic, and catalytic properties, making their applications an explosive growth during the past few decades [1–5]. Particularly, the outstanding performance of metal nanocrystals in catalytic applications has become the focus of "green chemistry" [5–8]. However, it should be noted that, although the metal nanocrystals usually exhibit favorable catalytic activities for certain reactions, most of them are difficult to commercialize for practical applications [9–12]. For example, the first-row transition metals cannot meet all the requirements for a given catalytic application due to their labile nature and insufficient reactivity profiles [9,10]. Especially the unsatisfactory stability caused by the dissolution of metal atoms during the catalysis process is a massive problem that severely hinders their practical applications [10,11]. The second- and third-row late transition metal, like Pt, Pd, Ru and Au has been widely exploited as the most effective catalyst in the field of electrocatalysis and organic transformation [7,8,12]. Nevertheless, the high price of these noble metals causes serious concerns in their potential large-scale applications. As well, their catalytic durability remains unsatisfactory for most commercial applications.

To resolve the above-stated issues, numerous efforts have been devoted to improving the catalytic performance of metal nanocatalysts *via* different strategies. In the past few decades, many strategies have been successfully developed to improve the catalytic performance of metal nanocrystals, including preparing bi- or poly-metallic alloys, constructing metal/support interaction, and manipulating the size, morphology, and crystalline phase of metal nanocrystals [5–7,13]. These strategies can efficiently modulate the catalytic property of metal nanocrystals and thus provide ways to generate efficient and stable nanocatalysts. Most recently, metal-nonmetal nanocrystals derived by filling nonmetal elements into host metals, such as metal hydrides [14–21], metal borides [22–25], metal carbides [26–33], metal nitrides [34–40], metal oxides [41–48], metal phosphides [49–55] and metal chalcogenides [56–60], have received increasing attention owing to their excellent catalytic performance in many important reactions. Indeed, the metal-nonmetal nanocrystals have diverse stoichiometries and phases, as well as specific physical-chemical properties associated with the type of nonmetallic elements. These advantages, combining with low cost and excellent corrosion resistance, making metal-nonmetal nanocrystals extensively

* Corresponding author.
E-mail address: jinm@mail.xjtu.edu.cn (M. Jin).

https://doi.org/10.1016/j.cclet.2021.03.041

explored as the most attractive candidates for noble metal nanocrystals in catalytic applications [14,57–60].

In this minireview, we will discuss recent advances in the synthesis of metal-nonmetal nanocrystals with diverse stoichiometries, morphologies, and their resulting performance as catalysts for a set of catalytic reactions. First, we review the latest reported metal-nonmetal nanocrystals and classified these nanocrystals into seven groups based on the type of nonmetallic elements, which are metal hydrides, metal borides, metal carbides, metal nitrides, metal oxides, metal phosphides, and metal chalcogenides (Fig. 1). We then present several examples to highlight the use of metal-nonmetal nanocrystals as catalysts in electro- and organic-catalytic reactions, including electrocatalytic methanol oxidation reaction (MOR), formic acid oxidation reaction (FAOR), oxygen reduction reaction (ORR), hydrogen evolution reaction (HER), oxygen evolution reaction (OER), CO_2 reduction reaction (CO_2RR), N_2 reduction reaction (NRR), catalytic hydrodesulfurization (HDS), hydrodenitrogenation (HDN), hydrodeoxygenation (HDO), hydroazidation, CO_2 hydrogenation, and semihydrogenation. Finally, we will propose some perspectives for the catalysis-driven rational design of metal-nonmetal nanocrystals. We hope this review could offer information on the research of metal-nonmetal nanocrystals timely and provide guidance for their applications in catalysis.

2. Classification and catalytic application of metal-nonmetal nanocrystals

2.1. Metal hydrides

Metal hydrides are a class of hydrogen compounds composed of metals and hydrogen elements. As the smallest of all atoms, hydrogen can diffuse into their host metals at extraordinary high mobility and reach the thermodynamic equilibrium in a short time, resulting in metal hydrides in which hydrogen occupies octahedral or tetrahedral interstitial sites of the metal lattices (Fig. 2a) [61]. The nature of metal-hydrogen bonding makes metal hydrides numerous unique physical and chemical properties, which are very different from those of their host metals. Specifically, the electrons from the inserted hydrogen atoms join the conduction band near the Fermi level of the host metal and increase the electron density as well, thereby affecting the electronic, magnetic, and optical properties of metal hydrides. On the other hand, the insertion of hydrogen into the interstitial sites of metals expands the crystal lattice and changes the mechanical properties of the metal hydrides.

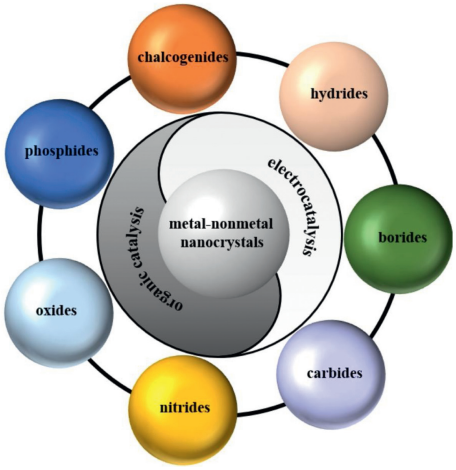

Fig. 1. Schematic illustration of various metal-nonmetal nanocrystals for electro- and organic-catalytic applications.

Most metal hydrides, such as LiH, NaH, MgH_2, CaH_2, AlH_3 and TiH_2 can be synthesized *via* a gas-solid method by directly reacting metals with hydrogen gas at elevated temperatures [62]. Due to the limited thermal stability of the resulting metal hydrides, hydrogenation synthesis of metal hydrides is usually carried out at moderate temperatures (< 500 °C). For some metal hydride phases with high coordination numbers or high metallic oxidation states, such as Sr_2MgH_6 and K_2PtH_6, the insertion of hydrogen needs to be combined with necessary high hydrogen pressure (up to 10 GPa). Besides gas-solid method, some other alternative approaches such as solution method, ion implantation, ball-milling, and electrochemical synthesis could also be used to synthesize metal hydrides, but they are not very widely used techniques and only for some specific metal hydrides owing to the difficulties encountered during their synthesis. For example, ZnH_2, K_2ReH_9 and PdH_x can be prepared through a solution route, while the preparation of CrH can be achieved *via* electrochemical synthesis. Additionally, the ion implantation and ball-milling in a hydrogen atmosphere can be used to prepare some hydrogen storage materials, such as $BaReH_9$, $LaNi_5H_6$, $FeTiH_{1.7}$ and Mg_2H_2 [62,63]. It is worth mentioning that many metal hydrides are sensitive to air and moisture and must be stored under an inert atmosphere. Metal hydrides, especially those containing heavy alkaline metals, are highly reactive and have to be kept in inert gas atmospheres [63].

In the past few decades, metal hydrides have been known as natural candidates for hydrogen storage materials. There have already been several books and reviews on metal hydrides, introducing the synthesis, characterizations, and hydrogen storage capabilities [64–67]. In this review, we mainly focus on the electrocatalysis and organic catalysis of metal hydrides, as the interest in catalytic applications of metal hydrides has grown dramatically in recent years. Metal-hydrogen bonds have been proven to play a critical role in catalytic processes [14–17]. For example, Ni-H bonds are found to be involved in many catalytic processes, such as electrocatalytic oxidation of H_2, Ni-containing enzyme (*e.g.*, NiFe hydrogenase and methyl-coenzyme M reductase) catalysis, suggesting the nickel hydrides to be the key component for the catalysis [14]. In another important industrial reaction, the ZrCo-catalyzed hydrogenation of CO_2, methane products were found to form on $ZrCoH_x$ in the course of hydrogen desorption but not on the pristine metals, meaning that the real catalyst is the hydrides [15]. LiH, NaH, KH, MgH_2 and CaH_2 can be used to crack ammonia into hydrogen and were able to perform the reaction under mild conditions [16]. More importantly, due to the feasibility of tailoring metal-hydrogen bond strengths by forming metal hydrides, the application of metal hydrides in electrocatalysis (*e.g.*, HER and NRR) and organic catalysis have recently attracted increasing attention [15,15,16,17].

Although the intrinsic activity of metal hydrides meets the criteria of superior catalysts, there are few examples in which metal hydrides are individually prepared into stable nanoparticles for catalytic reactions, especially as electrocatalysts. Until recently, metal hydride nanomaterials for electrocatalytic applications have been reported. The most typical example is the extensive research of PdH_x nanocrystals, which provide a breakthrough in the prospect of hydride electrocatalysis applications [18–21]. In 2015, Huang and coworkers prepared shape-controlled $PdH_{0.43}$ nanocrystals using a solution method with *N*,*N*-dimethylformide (DMF) as a hydrogen source (Fig. 2b) [18]. During the synthesis, the *in-situ* hydrogen gas generated by the catalytic decomposition of DMF can diffuse into Pd lattices to form $PdH_{0.43}$ nanocrystals. Remarkably, the obtained $PdH_{0.43}$ nanocrystals demonstrated high stability under ambient conditions and elevated temperatures, as well as strongly enhanced catalytic activities toward MOR. In

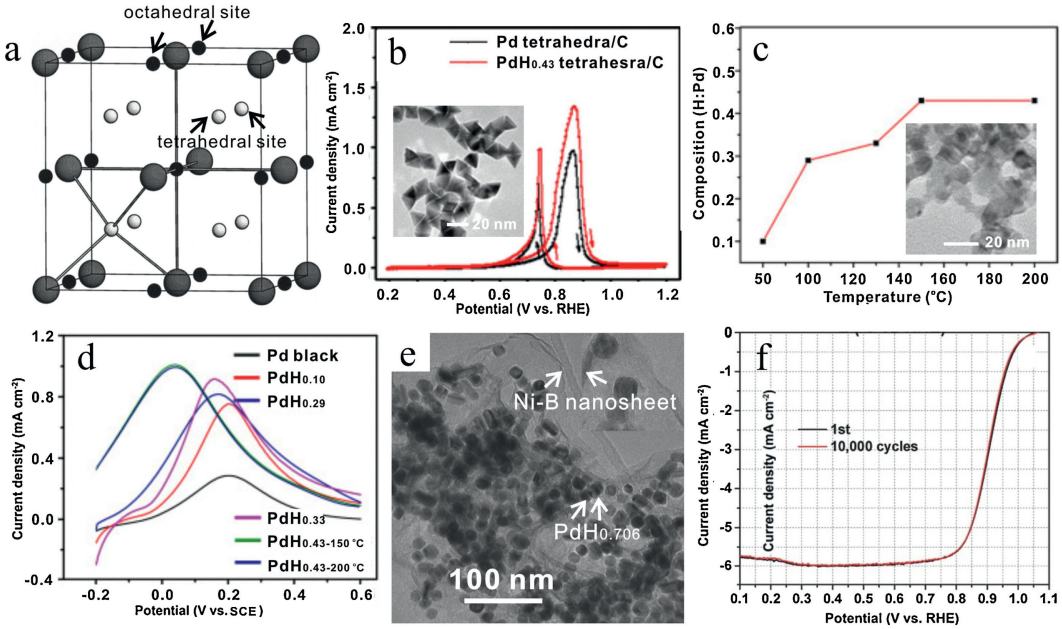

Fig. 2. (a) The position of hydrogen atoms in a representative Cu-type structure (cubic closet packed structure). Large spheres represent metal atoms, small filled spheres represent octahedral interstitial sites, and the small empty spheres represent the tetrahedral interstitial sites. Reprint with permission [61]. Copyright 2003, Elsevier. (b) Comparison of cyclic voltammetry (CV) curves for Pd nano-tetrahedra and $PdH_{0.43}$ nano-tetrahedra in 0.1 mol/L KOH and 0.1 mol/L methanol solution. Inset in (b) is the TEM image of $PdH_{0.43}$ nano-tetrahedra. Reprint with permission [18]. Copyright 2015, American Chemical Society. (c) Compositions of as-prepared PdH_x nanocatalysts obtained at different reaction temperatures and (d) the CV curves of Pd black and PdH_x nanocatalysts with different H contents in 0.25 mol/L HCOOH and 0.5 mol/L H_2SO_4 solution. Inset in (c) is the TEM image of obtained PdH_x nanocatalysts. Reprint with permission [20]. Copyright 2018, Elsevier. (e) TEM image of $PdH_{0.706}$@Ni-B composites and (f) their ORR polarization curves before and after 10,000 potential cycles in 0.1 mol/L $HClO_4$ solution. Reprint with permission [21]. Copyright 2017, Wiley-VCH.

another work, Xie *et al.* reported the successful synthesis of PdH_x nanocatalysts with controllable hydrogen contents by a solvothermal condition (Fig. 2c) [20]. Due to the downshift of the D-band center of Pd caused by the penetration of H, the binding strength between catalyst surface and reaction intermediates can be effectively modified, thereby improving the catalytic activity of the resulting PdH_x nanocrystals. When served as electrocatalysts for FAOR, the $PdH_{0.43}$ nanocrystals could exhibit an extraordinarily low peak potential of 0.04 V *vs.* saturated calomel electrode (SCE) and high mass activity of 1.06 A/mg (Fig. 2d), as well as the much-enhanced catalytic stability compared with commercial Pd black. $PdH_{0.706}$@Ni-B composites can be prepared by embedding $PdH_{0.706}$ nanocubes in NiB nanosheets, which were proven to be excellent ORR electrocatalysts in acidic medium (Figs. 2e and f) [21]. At 0.90 V *vs.* reversible hydrogen electrode (RHE), the mass activity of $PdH_{0.706}$@Ni-B composites reached 1.05 A/mg, which is nearly 5 times higher than that of commercial Pt/C catalyst. Moreover, there is a negligible loss in their catalytic activity after 10,000 potential cycles (Fig. 2f). Overall, these pathbreaking reports have led to the application of metal hydrides as electrocatalysts, and the current research on this aspect is still ongoing.

Given the primary position of hydrogen in the periodic table and many important properties of metal hydrides, the research on the synthesis of metal hydrides remains an important topic of chemical technology. We believe that more attention and efforts for the synthesis and application of metal hydrides will be paid in the future.

2.2. Metal borides

Metal borides represent another important class of binary or multiparty inorganic solids, often formed by the reaction between metal and boron, in which boron is the electronegative partner. Recently, metal borides have been reported to possess high activity, long-term stabilities, and cost-effectiveness in many electrocatalytic reactions. For example, CoB, NiB_x and MoB were found to exhibit excellent catalytic performance toward HER in a wide pH range, representing low-cost alternatives to noble metal-based electrocatalysts [68–70]. Therefore, metal borides have attracted considerable attention in recent years and a set of metal borides have been reported, such as NiB, CoB, MoB, FeB_2, TiB_2, VB_2 [68–72]. Conventionally, almost all metal borides can be synthesized *via* the solid-state reaction between metal and boron, such as those mentioned above. However, these solid-state reactions can only take place at high temperatures, in which case would undoubtedly lead to metal borides with large particle sizes, uncontrolled crystallization, and/or mixed phase products [73,74]. In this case, great efforts have been devoted to developing general and low-temperature methods for the preparation of metal borides in the past decades and new approaches such as reduction of metal salts or oxides with boron compounds have been successfully developed [23,72]. For example, Fokwa *et al.* reported a series of 3*d*-based metal borides, such as CoB, FeB, VB_2, NbB, NbB_2, MoB, WB and TaB_2 nanocrystals with well-defined morphology and small particles, which were obtained by the reaction of anhydrous metal chlorides and boron in the presence of reducing tin metal under low temperatures [72].

These new approaches enable us to produce a large number of metal borides and further extend our capability to manipulate their morphologies and stoichiometries. Both the morphology and stoichiometry could play key roles in determining the catalytic performance of metal borides. For example, it has been reported that metal borides show strong boron-dependency catalytic activities when served as electrocatalysts for HER [70,73,75]. α-MoB, β-MoB and MoB_2, which possess higher boron contents, would exhibit much higher HER activities than Mo_2B. Moreover, the H_2 generation rate using Co-B film catalyst is about 6 times higher than that of Co-B particle catalyst, showing a significant morphology effect [76]. On the other hand, filling boron atoms into metal lattices to form metal borides can further lead to lattice

strains within the metal borides, which may further endow the materials with superior catalytic properties. As been reported recently, FeB_2, Co_2B, Co-Ni-B and other metal borides nanocrystals have been proven to be excellent bifunctional electrocatalysts for overall water splitting [22,23,77]. Schuhmann and co-workers reported that the incorporation of boron elements in Co lattices can induce lattice strain in the crystal structure of Co metal and thus diminish the thermodynamic and kinetic barrier of the hydroxylation reaction, which is a rate-determining step in the OER (Fig. 3) [23]. As shown in Fig. 3c, only 1.6 V *vs.* RHE on inert support and 1.59 V *vs.* RHE on nitrogen-doped graphene (NG) are required for Co_2B-500 catalysts to achieve a current density of 10 mA/cm^2, which is the highest value for cobalt-based catalysts reported to date. Moreover, no activity loss can be observed after 60 h electrolysis, indicating the superior stability of Co_2B-500 toward OER (Fig. 3d). As a bifunctional electrocatalyst, Co_2B catalysts can also deliver high activities toward HER.

Water splitting devices with Co_2B-500 nanocrystals as anodic and cathodic catalysts can show a cell voltage of 1.81 V at 10 mA/cm^2. Cell voltages could be well maintained after 5000 cycles, implying that Co_2B-500 is a potentially very stable catalyst for water splitting (Figs. 3e and f). These examples demonstrate that metal borides can show excellent performance toward a set of electrocatalytic reactions, and could be applied as a type of low-cost alternatives for noble metal electrocatalysts. However, it is noteworthy that the applications of metal borides are far less extensive than metal carbide or metal phosphides. This is mainly due to the difficulties encountered in their synthetic process, which may need high temperature or pressure. In addition to electrocatalytic applications, metal borides have also been recognized as an important type of catalysts for organic reactions. Taking HDS reaction as an example, it has been found that Ni-B and Co-B can exhibit superior catalytic activities toward this reaction [24]. Ni-B nanocrystals can also be applied as active catalysts for syngas synthesis from the partial oxidation of methane and steam reforming [25,78], while Co-B nanocrystals can be used as efficient Fischer-Tropsch catalysts [79]. In addition to binary borides, ternary metal borides (*e.g.*, Ni-Mo-B and Co-Mo-B) have also been synthesized and reported, while some of them can exhibit extremely high activities for the HDO of bio-oil [80,81].

Compared with metal nanocrystals, metal borides can exhibit superior catalytic performance, mainly due to the strong host-guest electronic interaction between metal and subsurface boron atoms. Such electronic structure modification can also take effect on noble metal nanocrystals [82–84]. Recently, Cai and co-workers demonstrated that Pd-B (or B-doped Pd) can be prepared by reducing Na_2PdCl_4 with dimethylamine borane in the presence of H_2BO_3 and NH_4F [82]. These Pd-B nanocrystals can show much-enhanced activity toward hydrogen production from a mixed solution of formic acid and sodium formate at room temperature as compared with the commonly used Pd/C, Pd/Au and Pd/Ag catalysts. The turnover frequency (TOF) of Pd-B nanocrystals for H_2 production reaches 1184 h^{-1}, which is about 3 times higher than that of the commercial Pd/C catalyst. Real-time attenuated total reflection infrared (ATR-IR) spectroscopy revealed that the important role of boron filling in modifying the Pd surfaces to impede Co_{ad} accumulation.

As a group of important catalysts, noble metal nanocatalysts have shown their importance in our modern society, catalyzing numerous important reactions related to modern industry. Boron filling has shed light on the modification of noble metal nanocatalysts to achieve higher activities and/or better stabilities, but so far only Pd-B has ever been reported. More works on metal borides are still required, not only to develop efficient approaches for the synthesis of metal borides, but also to uncover the role of boron in improving their catalytic properties in important reactions.

2.3. Metal carbides

Metal carbides, which are composed of metal and carbon, are often described as interstitial compounds, with carbon atoms fit into the interstitial sites in metal lattices. Different from metal hydrides and borides, metal carbides would tend to show metallic

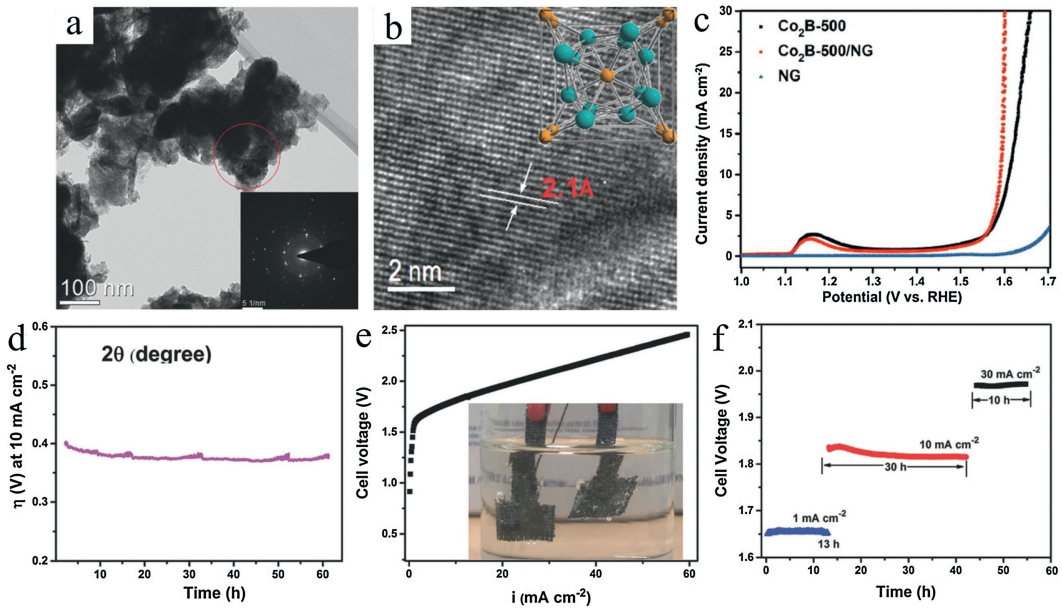

Fig. 3. (a) TEM image of Co_2B-500 catalyst with the SAED pattern of the circular marked region shown in the inset. (b) HRTEM image of Co_2B-500 catalyst with the inset showing the unit cell structure of Co_2B. The large blue spheres represent Co atoms, and the small orange spheres represent the B atoms. (c) LSV polarization curves of Co_2B-500, Co_2B-500/NG, and nitrogen-doped graphene in 0.1 mol/L KOH and (d) galvanostatic stability data of Co_2B-500 catalysts. (e) Complete water electrolysis in 3 mol/L KOH, the inset is the photographic image of the cell during electrolysis. (f) Chronopotentiometry stability data of Co_2B-500 catalysts at different current densities during electrolysis of water. Reprint with permission [23]. Copyright 2019, Wiley-VCH.

properties and can exhibit a range of stoichiometries. Some metal carbides have already been used as important industrial materials for a few hundred years, such as Fe-C. Thanks to the *in-situ* studies, researchers have found that metal carbides played key roles in some catalytic processes. Therefore, studies related to metal carbides have attracted intensive attention in recent years. By far, many metal carbides have been successfully prepared with size located at the nanoscale, which can be easily used as catalysts for electrocatalysis or organic catalysis [26–33,85–94]. The temperature-programmed reduction (TPR) method has been considered as the prominent strategy for the preparation of nanostructured metal carbides, which mainly involves the gas-solid reaction between related oxides and carburizing gases [85]. Carburizing gases mainly include CO, hydrocarbons (HC), and mixed gases such as CO/CO_2, CO/H_2 and HC/H_2. Various metal carbides, such as Mo_2C, Fe_3C, WC, TiC and NiC can be prepared by TPR method. Typically, pyrolysis of metal precursors (metallic salts or oxides) in organic solvents under inert atmospheres was also be used in the process of preparing metal carbides, even introducing various morphologies of products. For example, Mo_2C can be prepared by the pyrolysis of appropriate metal precursors under suitable conditions, which could result in different morphologies (nanowires or nanotubes) and composite catalysts (Mo_2C@carbon or Mo_2C@NCNT), and thus exhibit excellent HER catalytic properties [26,27,86,87]. Additionally, based on the confined carburization in the metal-organic frameworks (MOFs) matrix, researchers have developed a MOFs-assisted to prepare the MoC_x nano-octahedrons [88]. Recently, researchers have also developed many other synthetic approaches for preparing metal carbides with controllable stoichiometries and structures, such as hydrothermal/solvothermal synthesis. By treating pre-formed Pd nanocubes with glucose under hydrothermal conditions, our group have prepared a series of PdC_x nanocubes with controllable C/Pd atomic ratios from 0.04 to 0.18 [33].

Due to the strong binding of metal carbides towards a wide range of reactants and the high chemical and thermal stability, many metal carbides have been reported to show excellent electrocatalytic performance when served as catalysts or catalyst supports for noble metal nanocrystals [89]. Some metal carbides, which tend to show metallic properties, possess high electrical conductivity, and thus would benefit for their applications in electrocatalysis [90]. Besides metal-like conductivity, metal carbides with carbon atoms filled in the interstitial sites usually show different electronic structures relative to their parent metal nanocrystals due to the charge transfer between the metal and carbon atoms [91]. Therefore, one would be able to improve the catalytic performance of a given metal catalyst by finely controlling the electronic structures of metal carbides. By far, many metal carbides have been proven to be efficient catalysts for HER, with their intrinsic activities comparable to those of Group VIII noble metals [26–28,86,87]. For example, Peterson and co-workers have carried out steady-state polarization experiments and electronic structure calculations to reveal the catalytic activities of eight mono- and bimetallic carbides (WC, Mo_2C, NiC, TiC, Co_3C, Fe_3C and CoWC) toward HER and found these metal carbides to have activities higher than those of their parent metals [92].

Taking Mo_2C as a notable example, nanoporous Mo_2C nanowires (np-Mo_2C NWs), which were prepared by pyrolysis of MoO_x/amine hybrid precursor, can deliver a superior HER activity with a Tafel slope of ~53 mV/dec in acid solution due to the enriched nanoporosity and large reactive surface [86]. Besides, the catalytic current density could be well maintained at ~12 mA/cm^2 for 25 h of operation. Hierarchical β-Mo_2C nanotubes constructed from porous nanosheets have also been reported to facilitate the charge/mass transport during the electrochemical process, with an overpotential of only 112 mV (or 172 mV) at a current density of 10 mA/cm^2 in alkaline (or acidic) electrolytes [87]. Moreover, the stability of metal carbides can be improved by combining metal carbides with conductive supports, such as graphene and carbon nanotubes. For example, Mo_2C nanoparticles embedded in a carbon matrix (Mo_2C@carbon) or N-doped carbon nanotubes (Mo_2C-NCNT) can serve as highly active and stable HER electrocatalysts [26,27]. Similarly, other metal carbides, such as WC, W_2C and Fe_3C also possess superior catalytic activities for HER [28,92,93]. More interestingly, further stability studies revealed that WC can even exhibit enhanced stability in a wide pH range, especially under low pH conditions, which is another advantage for their practical applications [93]. In addition to HER, metal carbides were demonstrated to be efficient electrocatalysts for other fuel cell reactions, including FAOR, MOR and ORR [29,94]. For example,

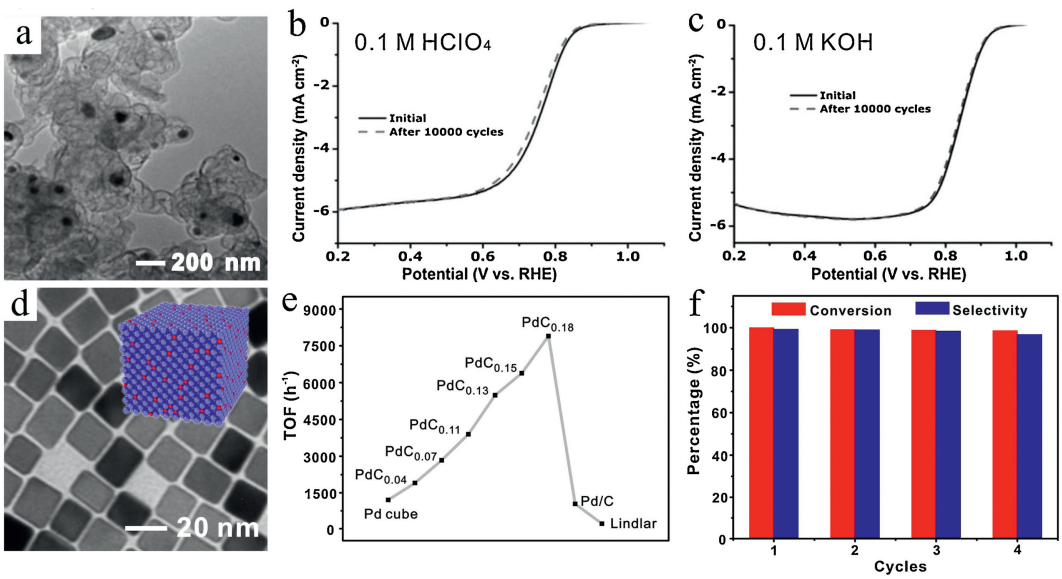

Fig. 4. (a) TEM image of Fe_3C/NG catalyst and their ORR polarization curves before and after 10,000 potential cycles in O_2-saturated 0.1 mol/L $HClO_4$ (b) and 0.1 mol/L KOH (c), respectively. Reprint with permission [94]. Copyright 2015, Wiley-VCH. (d) TEM image of $PdC_{0.18}$ nanocube catalyst. The inset in (d): crystal structure of PdC_x nanocube, the large blue spheres represent Pd atoms, and the small red spheres represent C atoms. (e) Plot of TOF over different related catalysts in hydrogenation of EB-H and (f) catalytic conversion and selectivity of $PdC_{0.18}$ nanocube catalyst during cycling. Reprint with permission [33]. Copyright 2019, Royal Society of Chemistry.

Xiao and co-workers demonstrated that Fe_3C encapsulated in graphitic layers (Fe_3C/NG) can act as an efficient and stable catalyst for ORR in both acidic and alkaline electrolytes, achieving highly competitive performance at a much lower cost compared with the state-of-the-art Pt/C catalysts (Figs. 4a-c) [94].

As we know, transition metals, such as W, Zr, Mo, Pd, Rh, are frequently used as catalysts for many reactions [5,6,33]. Filling carbon atoms into the metal lattices can be expected to further enhance the catalytic performances of these metal catalysts. Therefore, WC, ZrC, VC, Mo_2C, Cr_3C_3 and PdC_x nanoparticles have recently been fabricated and reported to show excellent catalytic activity or selectivity toward a set of catalytic reactions. For example, WC, ZrC, VC, Mo_2C, and Cr_3C_3 nanoparticles can serve as highly efficient catalysts for oxidation of CO and H_2 [30], Mo_2C and WC materials can be used as efficient catalysts for methane reforming with CO_2 [31], while Mo_2C catalyst for NH_3 decomposition and PdC_x for efficient semihydrogenation reaction [32,33]. Compared with their parent metal catalysts, metal carbides exhibit the enhanced catalytic activities and improved yields of target products. Most recently, our group have successfully prepared a set of PdC_x with controlled stoichiometries, including $PdC_{0.04}$, $PdC_{0.07}$, $PdC_{0.11}$, $PdC_{0.13}$, $PdC_{0.15}$ and $PdC_{0.18}$ (Fig. 4d) [33]. The interstitial C atoms in Pd lattices can increase the Fermi level of the Pd sites through the hybridization of the Pd d band with C s-p bands, leading to changes in the electronic structure. These changes can lower the adsorption energy of alkenes during the alkyne semihydrogenation process, resulting in much higher selectivity toward alkenes. As shown in Fig. 4e, $PdC_{0.18}$ nanocube catalysts exhibit a record-high TOF of 7896 h^{-1} for 4-ethynyl-1,1′-biphenyl (EB–H) semihydrogenation reaction, which is ~7.8 and ~38 times higher than that of the commercial Pd/C and Lindlar catalyst, respectively, as well as selectivity of > 99%. Such outstanding catalytic performance can be well maintained after 4 cycles (Fig. 4f). Based on the above conclusions, it should be noted that metal carbides with carbon atoms filled into the interstitial sites of metal lattices can act as one of the most likely alternatives for metal catalysts, serving as efficient catalysts in many catalytic reactions. Especially in the field of electrocatalysis and organic catalysis, metal carbides could be expected to fulfill the promise of efficient and fruitful catalysts and play the dominant role in inorganic catalysts.

2.4. Metal nitrides

Metal nitrides, which are composed of metal and nitrogen atoms, are also known as non-stoichiometric and interstitial compounds since nitrogen atoms would like to fill into the interstitial sites in metal lattices with various stoichiometries. However, due to the relatively larger electronegativity of nitrogen compared with carbon, the properties of metal nitrides are strongly dependent on the content of nitrogen. Taking conductivity, for example, metal nitride is highly conductive when the content of nitrogen is low, and the conductivity would gradually decrease with the increase of nitrogen content [95]. Therefore, the synthesis of metal nitrides with controllable nitrogen contents has become the main focus of many recent investigations. In general, the synthesis of metal nitrides involves similar experimental procedures with the TPR method for metal carbides except replacing the carburizing gases with pure NH_3, a mixture of NH_3 and inert gas or compounds that can produce NH_3 (*e.g.*, urea). In this process, metal nitrides, such as Mo-N, Fe-N, Co_4N, Ni_3N, NiMoN and W_2N nanocrystals can be prepared through the reaction between metal or metal precursors and NH_3 during the annealing process [34,35,37–39,96–98]. Some other methods such as hydrothermal synthesis was also applied to prepare PdN_x nanocrystals [40]. Due to the strong attraction of nitrogen for the metal atoms, most metal nitrides are often refractory materials that are of high thermal and stability and corrosion resistance [99–101]. The stability and corrosion resistance of metal nitrides can be attributed to the high energy of the triple bonds between metal and nitrogen atoms and simultaneously, most metal nitrides are more stable than their oxides and hydroxides [102,103].

Metal nitrides with low nitrogen contents would have superior electrical conductivities, showing metallic states with continuous conductivity near the Fermi level [104]. The poor conductivity of the electrocatalysts may strongly limit their catalytic performance

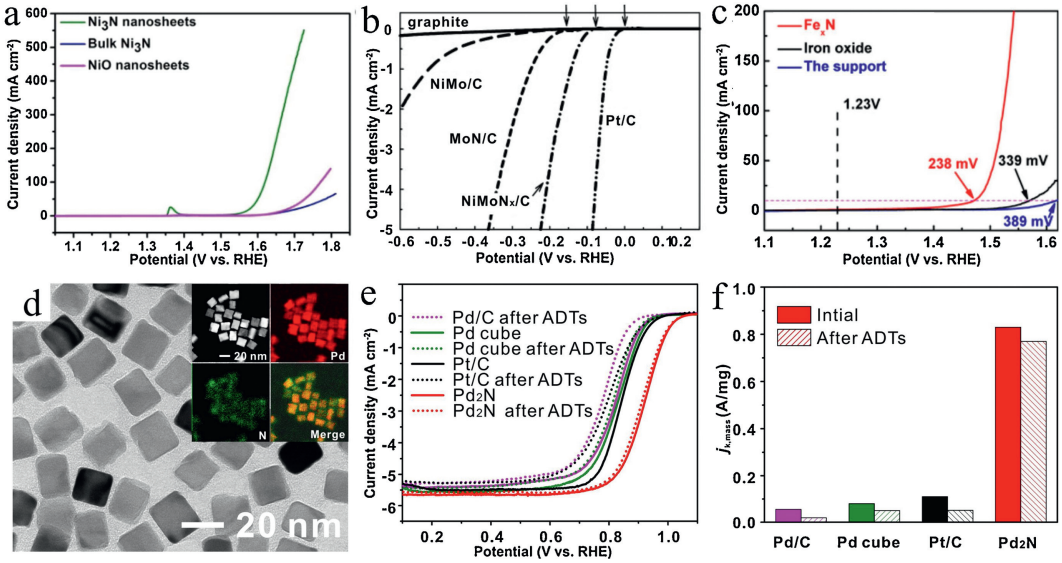

Fig. 5. (a) The comparison of normalized OER polarization curves of Ni_3N nanosheets, bulk Ni_3N, and NiO nanosheets catalysts in 1 mol/L KOH solution. Reprint with permission [37]. Copyright 2015, American Chemical Society. (b) The HER polarization curves of $NiMoN_x$/C and their component electrocatalyst, commercial Pt/C, and graphite in 0.1 mol/L $HClO_4$ solution. Reprint with permission [38]. Copyright 2012, Wiley-VCH. (c) OER polarization curves of as-prepared nanoporous Fe_xN film in comparison with iron oxide and support. Reprint with permission [39]. Copyright 2017, American Chemical Society. (d) The TEM image of the obtained Pd_2N nanocrystal catalysts. The inset in (d): HAADF-STEM image and relative EDS mappings of Pd_2N nanocrystal. (e) ORR polarization curves and (f) histogram of mass activities at 0.90 V *vs.* RHE of original Pd nanocubes, commercial Pd/C and Pt/C catalysts, and Pd_2N nanocrystals before and after ADTs of 10,000 cycles. Reprint with permission [40]. Copyright 2021, Royal Society of Chemistry.

due to the difficulties in electron transfer among the reactant, the catalyst and the electrode [95]. Therefore, metal nitrides with lower nitrogen contents could be expected to show higher activities than those with higher nitrogen contents toward electrocatalysis. As one of the notable examples, two-dimensional Ni_3N materials can be used as novel OER electrocatalysts (Fig. 5a) [37]. The excellent catalytic performance in terms of both activity and stability could be attributed to the superior electrical conductivity and the atomically disordered structure of two-dimensional Ni_3N. $NiMoN_x$ sheets, which consist of γ-Mo_2N and Ni_2Mo_3N phases, were also demonstrated to exhibit significantly enhanced HER activity compared with MoN and NiMo catalysts (Fig. 5b) [38]. Mo_2N nanocrystals can be used as highly stable and efficient electrocatalysts in NRR [98]. Fang and colleagues synthesized cubic Cu_3N nanocrystals by a facile one-phase process and demonstrated their high ORR electrocatalytic activity in alkaline media [36].

When further combined with certain supports, metal nitrides can deliver even higher activities and better stabilities during the electrochemical processes. For example, nanoporous Fe_xN film supported on three-dimensional highly conductive graphene/Ni foam was demonstrated to be highly active for OER (Fig. 5c) [39]. It should be noted here that Fe-N active sites can also weaken the adsorption energy of ORR intermediates and reduce the reaction barriers of potential limiting step, making Fe-N-C nanocrystals highly active for ORR [105]. Generally, electronic structures of the metal catalysts modified by forming metal-nitrogen bonds would lead to metal nitride electrocatalysts with better durability, economic efficiency, and higher activity than their parent metals [34–40,104]. In addition to electrocatalysis, metal nitrides can also act as efficient catalysts for many other reactions, such as CO_2 hydrogenation and HDN. As an important processing step in upgrading hydrocarbon feedstocks to commercially useful products, HDN has long been considering as one of the most important catalytic reactions in the industry [35]. Metal nitrides have been proven to show their outstanding capabilities in denitrogenating catalysis without saturation of the surrounding aromatic rings [34,35]. For example, by TPR of MoO_3 and NH_3, Mo nitrides can be prepared and show exceptional catalytic properties toward pyridine HDN, with much higher activities and better C—N bond hydrogenolysis selectivity than commercial sulfide Co-Mo hydrotreatment catalyst [34]. Hydrogenation of CO_2 into fuels and useful chemicals can also be accelerated by using metal nitrides as catalysts. Although this reaction can be catalyzed by metal catalysts, it should be mentioned that the catalytic activity can be significantly enhanced by incorporating nitrogen atoms into metal lattices. As a notable example, Zeng and co-workers have recently prepared Co_4N nanosheets by doping N into Co nanosheets [96]. The catalytic evaluation revealed that the TOF of CO_2 hydrogenation on Co_4N nanosheets is 64 times that of Co nanosheets, which is also higher than that of commercial Cu/ZnO/Al_2O_3 catalyst. Mechanistic studies suggested that Co_4N nanosheets were converted into Co_4NH_x by adsorbing H atoms, in which amido-hydrogen atoms can directly interact with CO_2 to form intermediate HCOO*. Besides, the adsorbed H_2O* can activate amido-hydrogen atoms through the interaction of hydrogen bonds, thereby promoting the hydrogenation process.

Although great success has been achieved in the synthesis of transition metal nitrides, there are relatively few reports on the synthesis of noble metal nitrides due to the unreactive nature of the most common nitrogen regents and strong bonding between metal atoms. Not until recently, Cao and co-workers reported the successful synthesis of AgN_3 nanocatalysts and found the AgN_3 to be a highly robust catalyst for hydroazidation of terminal alkynes [106]. Even with loading as low as 5 mol%, AgN_3 was still highly efficient, suggesting the excellent catalytic property of noble metal nitrides. Raymond E. Schaak has recently demonstrated the preparation of ternary metal nitrides Cu_3PdN through reacting copper(II) nitrate and palladium(II) acetylacetonate in 1-octadecene with oleylamine at 240 °C [107]. When served as electrocatalysts for ORR, Cu_3PdN nanoparticles can deliver much higher mass activity and better stability than both Pd and Cu_3N catalysts, showing the great enhancement by filling nitrogen into metal lattices. Most recently, our group has successfully prepared PdN_x nanocrystals ($x \leq 0.5$) with controllable stoichiometries by incorporating nitrogen atoms derived from the hydrothermal decomposition of urea into Pd nanocubes (Fig. 5d) [40]. Importantly, the obtained PdN_x nanocrystals can deliver superior catalytic performance for a wide range of fuel cell reactions, such as cathodic ORR, anodic FAOR and MOR, far surpassing the commercial Pd/C and Pt/C catalysts. Especially for ORR in alkaline electrolyte, the Pd_2N nanocrystals showed a mass activity as high as 0.83 A/mg at 0.90 V *vs.* RHE, outperforming most of the Pd-based electrocatalysts reported previously. Moreover, as shown in Figs. 5e and f, Pd_2N nanocrystals can exhibit excellent cycling stability toward ORR with activity decay only ~9% after accelerated durability tests (ADTs) of 10,000 cycles, suggesting a huge impact of nitrogen atoms on enhancing the stability of noble metal nanocatalysts. Despite these successes, it should be noted that noble metal nitrides are notoriously difficult to be prepared into nanoparticles. Therefore, in the future, it is highly encouraged to develop the efficient synthesis of noble metal nitrides nanocrystals for efficient electrocatalysts applications.

2.5. Metal oxides

Up-to-date, metal oxides have been regarded as one of the most well-known inorganic compounds to scientists, which contain the most extensive types and can be prepared by nearly all chemical synthesis methods. The easiest way to prepare metal oxides is calcination the commercial precursors refined from natural, for example, using relatively metal nitrates or carbonates to prepare Mn, Zn, La and Ce associated oxides, and using metal ammonium salts for the preparation of V, Mo and W oxides [108]. The most common method for obtaining metal oxides is to precipitate oxide precursors in an aqueous solution and/or subsequently perform thermal activation. In this method, the as-prepared metal oxides could be able to inherit the morphological characteristics from their precursors, which makes precipitation method an easy way for preparing variants of the same oxide, regardless of particle sizes and shapes. For example, alumina catalysts with different morphologies and crystallizations can be synthesize by adjusting the characteristics of the different aluminum hydroxides [108]. In addition, metal oxides of the first line of transition metals, such as Mn, Fe, Co, Ni, Cu and Zn oxides can also be prepared *via* a solvothermal synthesis. Nowadays, owning to the huge progress in nanoscience, researchers have developed many other excellent strategies for preparing metal oxides nanocrystals, which can exhibit unique stoichiometries and morphologies. For example, NiO thin film can be prepared *via* the use of sol-gel method, WO_3 nanowires can be synthesized by a vapor transport method, ZnO nanocrystalline thin film is made of spray pyrolysis and SnO_2 nanowires are able to prepare through thermal evaporation [109]. As for the applications of metal oxides, it has been associated with a variety of brand-new developments and many advanced technologies in this field. In terms of catalytic applications, metal oxides cover the majority of catalyst families in the industrially, involving silica, alumina, TiO_2, ZnO, ZrO_2, perovskites and so on [110–112]. Most of them are very important heterogeneous catalysts and involve in many important chemical reactions, including petrochemicals, intermediates, fine chemical and biomass transformation reactions. For example, V oxides are being

developed as catalysts for fuel production [41], ZnO-Al_2O_3 catalysts are extremely crucial for the biomass conversion reactions, and $CuMnO_2$ and $CoFeO_x$ can efficiently catalyze the gas-phase partial oxidation of hydrocarbons [42,43]. Besides the high-activity in organic catalytic reactions, in the past few decades, metal oxides have also shown high efficiency and great potential in electrocatalytic applications [44–48]. Some noble metal oxides are even considered as members of the most durable and active water oxidation catalyst owing to their high electrocatalytic performance toward OER in both acidic and alkaline solution, such as IrO_2 and RuO_2 [113,114]. Moreover, some other metal oxides have demonstrated noble metal-like catalytic properties in many reactions. For example, it was reported that the ABO_3 (A = alkaline earth, B = transition metal) perovskite-based metal oxides and spinel oxides exhibit a high OER rate, and some even surpass the performance of benchmark noble metal OER catalysts, which is of great significance in energy storage and conversion system [47]. Table 1 listed the kinetic parameters of the important and representative metal oxide electrocatalysts toward OER, suggesting that they are low-cost alternatives to noble metal-based electrocatalysts [44,113–121].

To further obtain high-performance metal oxide electrocatalysts, researchers are committed to constructing metal oxides with specific nanostructures, which can facilitate exposure of a large number of surface-active sites. Taking MoO_2 as an example, Jin and co-workers have demonstrated that porous MoO_2 nanosheets can be used as bifunctional electrocatalysts for overall water splitting in alkaline media [44]. As reported, porous MoO_2 nanosheets catalysts only need a cell voltage of 1.53 V to reach a water-splitting current density of 10 mA/cm^2. In another work, the nanoflower-like MoO_2 on nickel foam only needs about 55 and 80 mV overpotentials to achieve current densities of 10 and 20 mA/cm^2, respectively, showing an excellent HER activity [45]. In addition, thanks to the doping of Co/N into MoO_2, Co-*N*-doped MoO_2 nanowires exhibited high ORR catalytic activity and outstanding HER performance with a low overpotential, high electrochemical activity and robust stability in alkaline media [46]. These examples clearly demonstrate that the specific nanostructures of metal oxides can increase the surface-active sites, and thus improve their catalytic activity. It is worth noting that the conductivity of metal oxides is usually much lower compared with metal catalysts, which is unfavorable for the charge transfer in the electrocatalysis process. Therefore, some metal materials or carbon-derived materials have been usually used as support of metal oxides to improve their electronic conductibility, just like the abovementioned hybridization of MoO_2 nanoflower on Ni foam. As another example, Tong *et al*. reported an efficient bifunctional electrocatalyst for OER and ORR by firmly coupling CoO_x nanoparticles with B, N-decorated graphene [122]. They proposed that the superior performance resulted from a strong bridging Co-N-C bond between CoO_x and graphene, which promoted electron transfer capability and provided highly active sites of CoO_x catalysts.

Table 1
The OER performances of representative metal oxides electrocatalysts.

Catalyst	Electrolyte	η_{10} (mV) [a]	Tafel slope (mV/dec)	Ref.
RuO_2	0.5 mol/L KOH	310	108.8	[113]
IrO_2	1 mol/L KOH	338	47	[114]
CoO_x	1 mol/L KOH	260	–	[115]
Co_3O_4	1 mol/L KOH	290	72	[116]
Ru@RuO_2	0.1 mol/L KOH	320	86	[117]
Mn-RuO_2	0.5 mol/L H_2SO_4	158	42.94	[118]
Fe-NiO	0.5 mol/L KOH	297	37	[119]
MoO_2	1 mol/L KOH	1490	54	[44]
$ZnCo_2O_4$	0.1 mol/L KOH	350	70.6	[120]
$LiCoO_2$	1 mol/L KOH	430	48	[121]

[a] η_{10} is the potential (*vs*. RHE) to achieve the current density of 10 mA/cm^2.

Table 2
HER performance of different metal phosphides.

Catalyst	Electrolyte	η_{10} (mV) [a]	Tafel slope (mV/dec)	Ref.
Ni_2P	1 mol/L H_2SO_4	42	38	[49]
Ni_2P	1 mol/L NaOH	69	118	[49]
Ni_5P_4	1 mol/L H_2SO_4	23	33	[49]
Ni_5P_4	1 mol/L NaOH	49	98	[49]
CoP	0.5 mol/L H_2SO_4	75	50	[51]
Co_2P	0.5 mol/L H_2SO_4	95	45	[51]
WP	0.5 mol/L H_2SO_4	130	69	[52]
WP	1 mol/L KOH	150	102	[52]
Ni_2P	0.5 mol/L H_2SO_4	45	46	[131]
$Ni_{12}P_5$	0.5 mol/L H_2SO_4	208	75	[133]
Ni_5P_4	0.5 mol/L H_2SO_4	118	42	[133]
CoP	0.5 mol/L H_2SO_4	85	50	[134]
CoP	0.5 mol/L H_2SO_4	67	51	[135]
CoP	1 mol/L KOH	209	129	[135]
FeP	0.5 mol/L H_2SO_4	58	45	[138]
FeP	1 mol/L KOH	218	146	[138]
FeP	0.5 mol/L H_2SO_4	52	49	[139]
MoP	0.5 mol/L H_2SO_4	η_{30} = 180	54	[143]
Mo_3P	0.5 mol/L H_2SO_4	500	147	[143]

[a] η_{10} is the potential (*vs*. RHE) to achieve the current density of 10 mA/cm^2.

Even though considerable progress has been acquired in the field of fabrication of metal oxides for catalytic applications, many questions should be addressed for their practical applications. In particular, more attention should be focused to improve the conductivity and catalytic stability of metal oxides, which are essential for the development of more efficient organic and electrocatalytic applications.

2.6. Metal phosphides

A metal phosphide, which consists of metal and phosphorus atoms, usually have metallic properties, and thus could be used as catalysts for electrocatalysis and organic reactions. By far, there have already been hundreds of metal phosphides synthesized and investigated on the nanoscale. The synthesis of metal phosphides nanostructures is much more difficult than that of carbides and nitrides and usually contains the use of toxic phosphorus source. The representative synthesis strategies for metal phosphides include the traditional solid-state method, gas-solid way, and solvothermal synthesis. The traditional solid-state method refers to direct reactions of red/white phosphorus and metals at a high temperature and under an inert atmosphere or vacuum. Using this approach, many metal phosphides such as CoP, NiP, FeP and MoP can be routinely accessed in high purity and on a large scale [123,124]. To accelerate the diffusion of the elements in the solid states, long reaction times and high temperatures would be required for the synthesis of metal phosphides by the solid-state method. The gas-solid way mainly depends on the PH_3 gas or the phosphates (such as $NH_4H_2PO_2$ or NaH_2PO_2) which can *in situ* generate PH_3 during heating process [125–127]. The PH_3 gas can directly react with metal precursors (such as metal oxide, hydroxides, salts, or metal-organic frames) to form metal phosphides nanocrystals under an atmosphere condition. For example, some important catalysts, such as FeP, Ni_2P, CoP, WP_2 and Cu_3P could be obtained *via* gas-solid strategies. Solvothermal synthesis usually uses organic phosphines, such as tri-*n*-octylphosphine (TOP), tri-*n*-octylphosphine oxide (TOPO) or triphenylphosphine (TPP) as phosphorus sources. The C–P covalent bond of organic phosphines can be easily broken at a temperature around 200 °C and thus release phosphorus. The phosphorus then reacts with the metals during the reaction to form a series of metal

phosphides such as Ni_2P_5, Ni_2P, Co_2P and WP [126]. Compared with the solid-state method and gas-solid method, solvothermal synthesis can prepare metal phosphides with controlled sizes or morphologies and can be carried out at a much lower temperature, so that solvothermal synthesis has been widely adopted for the preparation of metal phosphide nanocrystals in recent years. For example, our group has successfully converted 5 nm-Pt nanoparticles into Pt_2P nanocrystals by using TOP as a phosphorus [128]. More interestingly, many studies showed that metal phosphide nanocrystals can be prepared into hollow structures *via* solvothermal synthesis due to the Kirkendall effect [129,130].

Metal phosphides can exhibit superior catalytic performance toward an array of reactions compared with their parent metals, and both the metal phosphides and metals have similar conductivity, which could benefit for their catalytic applications in electrocatalysis. To date, a large number of metal phosphides have been reported, such as Ni_2P [49,50,131–133], Ni_5P_4 [49,133], CoP [50,51,134–136], Co_2P [51,137], FeP [138,139], Fe_2P [50,138,139], MoP [50,136,139,140], WP [50,52,137], Cu_3P [53], AgP_2 [141], Pt_2P [128], and demonstrated to show excellent catalytic performance in a set of reactions. For example, many metal-rich phosphides can exhibit excellent activity and stability for catalytic hydrogenation reactions, including HDS, HDN, and HDO reactions [50,132,137], since hydrogen can adsorb or desorb reversibly on the surface of metal phosphides. All of the MoP, WP, Fe_2P, CoP and Ni_2P have been reported to show excellent performance in HDS and HDN, with Ni_2P proving to be the most active. Oyama's review has already comprehensively covered the major development of these transition metal phosphides in hydroprocessing catalysis [50]. Besides hydrogenation reactions, metal phosphides have recently been proven to be efficient electrocatalysis, especially for HER. The catalytic performance of a given catalyst for HER and hydrogenation reaction both strongly depends on the reversibly associating and dissociating hydrogen atom, implying that metal phosphides should be also active for HER [142]. Table 2 has listed the recent superior catalytic performance achieved for HER on metal phosphides. More interestingly, some metal phosphides can even show high catalytic activity and stability toward HER in a wide pH range. For example, Ni_2P, Ni_5P_4, FeP, CoP and WP can exhibit excellent performance both under acidic and alkaline conditions [49,5,135,138]. The feasibility under a wide pH range makes them great potential to cooperate with OER catalysts for efficient overall water splitting reaction. Recently, Liu and coworkers demonstrated that CoP nanosheets arrays on carbon cloth can be used as a bifunctional water-splitting catalyst with high activity and durability in alkaline and neutral media [54]. Song's group prepared MoP/Ni_2P nanocrystals on three-dimensional Ni foam and found that these bimetallic phosphides can exhibit superior catalytic performance for OER and HER in alkaline electrolytes [55]. Importantly, it can be seen from Table 2 that metal phosphides with higher phosphorus content usually exhibit higher HER activity than those with lower phosphorus content. Specifically, in Ni-P, Co-P and Mo-P systems, the P-rich phases show much lower overpotentials and smaller Tafel slopes in either acidic or alkaline solutions. For instance, Ni_5P_4, CoP and MoP show higher activity than Ni_2P ($Ni_{12}P_5$), Co_2P and Mo_3P, respectively [49,51,133,143]. It is also worth noting that metal phosphides are an important class of compounds with metalloid characteristics and good electrical conductivity, even some metal-rich phosphides can exhibit superconductivity, which is beneficial for their electrocatalytic applications [144].

In recent years, noble metal phosphides have attracted enormous research interests purposed for further improving the catalytic performance of noble metal catalysts and reduce the mass loadings of these expensive noble metals [128,139,145,146]. Ag has been frequently used as benchmarked electrocatalysts for CO_2 to CO conversion but the high overpotential has largely limited the efficiency. Impressively, Li and co-workers have recently demonstrated that more than 3-fold reduction in overpotential can be achieved by filling P into Ag lattices to form AgP_2 [141]. Fig. 6a indicates the successful preparation of AgP_2 with size around 3.5 nm through a solvothermal synthesis. For CO_2 electrocatalytic reduction, the onset potential for initial CO generation on AgP_2 nanoparticles is −0.22 V *vs.* RHE, while it is −0.59 V on Ag nanoparticles with similar size (Fig. 6b). Density functional theory (DFT) reveals that the HER process can proceed *via* phosphorus sites, and the AgP_2 (111) surface has phosphorus sites with free energy for atomic hydrogen adsorption (ΔG_{H^*}) of 0.036 and −0.039 eV. The strong adsorption of H* on phosphorus sites can effectively suppress the HER rate, while the adsorbed H* could also be delivered to the adsorbed carbon species on adjunct silver sites to promote the hydrogenation reaction [141]. This study suggests the key role of phosphorus alloying on the enhancement of catalytic performance of noble metal catalysts. Most recently, our group demonstrates the successful synthesis of a new type of metal phosphide, Pt_2P nanocrystals, by treating Pt nanoparticles with TOP at 300 °C for 3 h (Fig. 6c) [128].

After filling phosphorus into Pt lattices, the catalytic performance of Pt catalysts can be markedly enhanced by factors of 10.3 in mass activity and 10.2 in specific activity, respectively. The durability test further demonstrated the superior stability of Pt_2P nanoparticles relative to Pt nanoparticles, with a drop of 9.1% in mass activity in the acidic medium after 30,000 potential cycles, showing another advantage of the noble metal phosphides (Fig. 6d). As been demonstrated, the catalytic performance of noble metal catalysts can be significantly improved toward electrocatalysis in terms of both activity and stability by filling phosphorus atoms. Later, Sun and co-workers reported that PdP_2 nanoparticles loaded on reduced graphene oxide (PdP_2-rGO) can be prepared by a modified high-temperature solid-state method *via* the reaction between Pd-GO and red phosphorus at 900 °C for three days [145]. The prepared PdP_2-rGO can reduce the energy

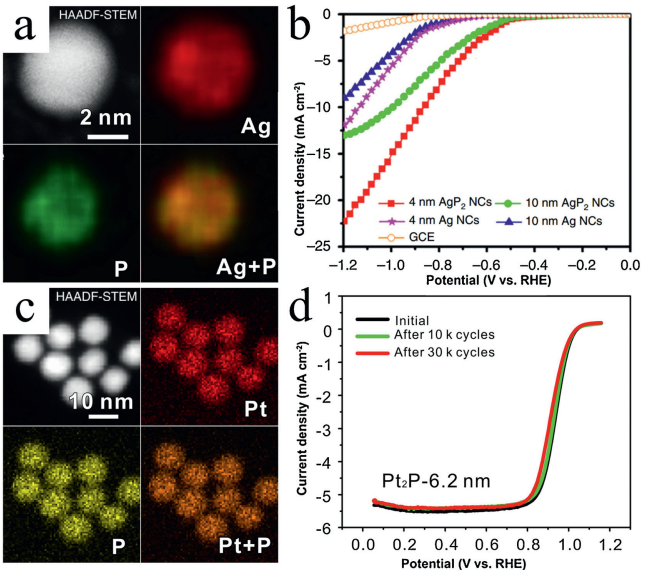

Fig. 6. The structural characterization and catalytic performance of noble metal phosphides nanocatalysts. (a) The HAADF-STEM and relative elemental mappings of AgP_2 nanocrystals and (b) comparison of LSV polarization curves of Ag and AgP_2 nanocatalysts in electrocatalytic CO_2 reduction reaction. Reprint with permission [141]. Copyright 2019, Nature. (c) The HAADF-STEM image and relative EDS mappings of Pt_2P nanocrystal catalysts and (d) their ORR polarization curves before and after 10,000 and 30,000 cycles. Reprint with permission [128]. Copyright 2019, American Chemical Society.

barrier required for N_2 activation and the subsequent hydrogenation process, making PdP_2 the high-performance NRR electrocatalysts for ambient N_2-to-NH_3 conversion with excellent selectivity.

Incorporation of phosphorus into metal lattices represents one of the most effective ways to tailor the electronic structure and surface properties of metal catalysts. The binding strength of reaction intermediates adsorbed on active metal sites can be regulated, thereby enhancing the catalytic activities. While the above-listed noble metal phosphides, including AgP_2, Pt_2P and PdP_2 nanoparticles, are proven to be attractive catalysts for electrocatalysis, it is still a tremendous challenge in the preparation of noble metal phosphides due to the lack of synthetic methods to fill phosphorus into noble metal lattices. Therefore, it is urgent to develop effective synthetic approaches for the preparation of noble metal phosphides. More importantly, a deep understanding of how phosphorus affects the catalytic efficiency, stability, and/or even selectivity of a noble metal catalyst toward specific catalytic reactions would benefit the rational-design of high-performance catalysts. In this case, a synthetic approach that can further regulate the stoichiometry of noble metal and phosphorus elements is highly desirable and has yet not been achieved by far.

2.7. Metal chalcogenides

Metal chalcogenide is known as a compound composed of metal and chalcogen elements, mainly including metal sulfide, metal selenide, and metal telluride. Although metal chalcogenides usually have simple stoichiometries similar to metal oxides, such as 1:1 and 1:2 for transition metal chalcogenides, it should be mentioned that metal chalcogenides with other stoichiometries have also been frequently reported in recent years with typical examples include metal-rich phases (*e.g.*, M_xS) of extensive metal-metal bonding and chalcogenide-rich phases (*e.g.*, M_2S_7 and M_2S_9) of extensive chalcogen-chalcogen bonding [147–156]. Compared with the chalcogenide-rich phases, metal-rich chalcogenides possess much higher conductivity, which can greatly accelerate the electron transfer during electrocatalysis and thus enhance the catalytic performance of metal chalcogenides for electrocatalysis [147]. By far, there have been many synthetic approaches reported in the literature for metal chalcogenides, including the solid-state method, molten flux synthesis, and hydro(solvo)thermal preparations [148–150]. Similar to the synthesis of metal phosphides, synthesis of metal chalcogenides *via* solid-state method requires a high temperature (usually higher than 600 °C) to activate the solid-solid diffusion and initiate the reaction between metal precursors and alkali-metal chalcogenides. However, it is extremely difficult to prepare the desired metal chalcogenides with well-designed sizes and structures *via* the solid-state method owing to the limitations in kinetic control of the reactions at high temperatures. Compared with the solid-state method, molten flux and hydro-(solvo)thermal synthesis can yield finely dispersed metal chalcogenides nanoparticles with well-defined sizes and morphologies through the reactions between metal precursors and alkali-metal sulfides or covalent sulfiding agents in molten salts or polar organic solvents. For example, Co-based sulfides with varying S content such as CoS, CoS_2, Co_3S_4 and Co_9S_8 have been prepared by solvothermal methods and reported with different morphologies [149,151]. These two approaches have been recognized as the most powerful synthetic methods that can be used to prepare metal chalcogenides with metastable phases, such as low dimensional metal chalcogenides, which are not accessible at high synthetic temperatures.

The physicochemical properties of metal chalcogenides, such as conductivity and thermal stability can be regulated by tailoring the stoichiometry and morphology. As we have concluded at the beginning of this part, metal chalcogenides can be prepared as metal-rich phases, in which case metal chalcogenides would exhibit extensive metal-metal bonds and thus high electrical conductivity could be expected. Therefore, many metal-rich chalcogenides have been reported to show excellent catalytic performance in electrocatalysis. Taking HER for example, a large number of metal-rich sulfides, such as Ni_3S_2, CoS and Cu_2S have been reported to exhibit superior catalytic activities and low overpotentials owing to their high electrical conductivities [152–154].

Table 3 provides a summary of recent superior HER electrocatalytic performance achieved on these metal chalcogenides. It has been highlighted that many metal sulfides and selenides, such as FeS, FeS_2, CoS, CoS_2, NiS_2, Ni_3S_2, NiSe and $CoSe_2$ are the ones frequently reported for the HER, representing promising alternatives to noble metal-based electrocatalysts [157–167]. Among them, the chalcogenide-rich compounds, on the other hand, are often hybridized with conductive supports and then applied as catalysts for electrocatalysis, providing an overall high electrical conductivity and sintering resistance. For example, the beaded-stream-like $CoSe_2$ nanoneedles on Ti foil ($CoSe_2$-BSND/Ti) were prepared by treating Co_3O_4 nanoneedles array with Se vapor, which could exhibit superior electrocatalytic performance toward HER with a small overpotential and long-term stability in the acidic electrolyte [56]. The excellent performance could be attributed to the unique three-dimensional conductive hierarchical structure which can provide highly accessible active sites, improved charge transfer kinetics, and attractive force between water and catalysts surface. In addition to the HER, metal chalcogenides are also promising candidates as efficient electrocatalyst for the OER. Taking $CoSe_2$ as a notable example, as reported, the $CoSe_2$ ultrathin nanosheets containing a large number of Co vacancies which served as active sites to efficiently catalyst the reaction, manifesting an OER overpotential as low as 0.32 V at 10 mA/cm^2 in alkaline medium [168]. As reported, it is also allowed to combine hybridization methods and heteroatom doping to further improve the OER performance of $CoSe_2$ electrocatalysts. For example, Mn-modulated $CoSe_2$ nanosheets exhibited a 5.8-fold enhancement in electrocatalytic activity relative to $CoSe_2$ (Figs. 7a and b) [169]. Moreover, precious metals such as Au and Ag are often used to regulate the electronic structure and electrical conductivity of $CoSe_2$ to constructure composite catalysts (such as Au/$CoSe_2$ and Ag-$CoSe_2$) with better OER catalytic performance [170,171].

The co-doping of nonmetallic atoms in metal nanocrystals is usually achieved by doping other nonmetallic atoms in metal chalcogenides, which has proven to be another effective strategy to improve their electrocatalytic activity [58,60,172–174]. According to earlier reports, nanostructured MoS_2 and WS_2 with exposed edges have emerged as promising HER electrocatalyst [57]. To

Table 3
Comparison of the HER performance with recently reported metal chalcogenides electrocatalysts.

Catalyst	Electrolyte	η_{10} (mV) [a]	Tafel slope (mV/dec)	Ref.
FeS_2	0.5 mol/L H_2SO_4	217	56.4	[157]
CoS_2	0.5 mol/L H_2SO_4	128	52	[158]
NiS	1 mol/L KOH	150	83	[159]
FeNiS	0.5 mol/L H_2SO_4	105	40	[160]
Co_3S_4	0.5 mol/L H_2SO_4	140	70	[161]
Ni_3Se_2	1 mol/L KOH	70	82	[162]
MoS_2/$CoSe_2$	0.5 mol/L H_2SO_4	68	36	[163]
$CoSe_2$	0.5 mol/L H_2SO_4	137	40	[164]
NiSe	1 mol/L KOH	96	120	[165]
$Co_{0.13}Ni_{0.87}Se_2$	1 mol/L KOH	64	63	[166]
CoPSe	0.5 mol/L H_2SO_4	370	46	[167]

[a] η_{10} is the potential (*vs.* RHE) to achieve the current density of 10 mA/cm^2.

further improve their performance, Xie's group prepared the oxygen-incorporated MoS_2 ultrathin nanosheets (O-MoS_2 NSs) *via* a hydrothermal method (Fig. 7c) [60]. The as-prepared O-MoS_2 NSs showed a low onset overpotential of 120 mV, extremely large cathodic current density, and excellent stability toward HER (Fig. 7d). The report reveals that the superior electrocatalytic performance benefited from the increased active sites provided by the disordered structure and the intrinsic conductivity improved by the incorporation of oxygen. In another work, Zeng's group constructed MoS_2-BP (black phosphorus) nanosheets through deposition of MoS_2 flakes on BP nanosheets [172]. Due to the electron donation of BP, the MoS_2-BP nanosheets exhibited enhanced HER catalytic activity in acidic solution, which was 22 times higher than that of MoS_2. Moreover, the N-doped Co_9S_8 on graphene supports (N-Co_9S_8/G) obtained by NH_3 plasma treatment of Co_9S_8/G can be applied as an advanced bifunctional electrocatalyst for ORR and OER in alkaline media, where their ORR performance is close to that of commercial Pt/C catalyst (Figs. 7e and f) [58]. It was proposed that the N-doping and etching of Co_9S_8/G were proceeded simultaneously, which could efficiently adjust the electronic properties of the catalyst and expose more electrocatalyst active sites, thereby improving the ORR and OER performance greatly. These fruitful results make metal chalcogenides competitive potential catalysts in the field of electrocatalysis.

In addition to electrocatalysis, MoS_2, NbS_2, ReS_2, RuS_2 and Co_9S_8 have also been proven to be highly affordable catalysts for hydrotreating reactions, such as HDS, HDN, and HYD reactions [155]. For example, thiol-treated Pd catalysts displayed excellent catalytic selectivity and activity toward the semihydrogenation of internal alkynyls [156]. It is also worth noting that metal chalcogenides are considered as promising alternative electrode materials in lithium/sodium-ion batteries and supercapacitors as well. Apart from the low cost, earth abundance, and convenience for fabrication, metal chalcogenides have a much higher theoretical capacity compared with traditional graphite for energy storage systems. Recently, Huang and coworkers proved that the theoretical specific capacity of FeS_2 would be even higher than that of $LiMO_2$ intercalation cathodes for lithium-ion batteries [175].

More interestingly, metal chalcogenides have attracted tremendous attention recently due to their low-dimensional metastable structures, as well as their recently discovered outstanding catalytic capabilities in photocatalysis, electrocatalysis, and organic catalysis [176,177]. For example, metal chalcogenides can be fabricated into two-dimensional morphologies, which would show interesting physical phenomena such as the quantum spin Hall effect, valley polarization, and two-dimensional superconductivity [178–180]. By far, hundreds of two-dimensional metal chalcogenides have been reported, including binary compounds and alloys [151]. These two-dimensional metal chalcogenides can be prepared *via* sulfurization, selenization, and tellurization of metals and metal compounds in organic solvents or molten salts.

3. Conclusions and perspectives

Over the past few decades, metal-nonmetal nanocrystals have stood out as one of the most effective catalysts because of their outstanding catalytic performance. This review provides an overview of recent progress in metal-nonmetal nanocrystals, including metal hydrides, borides, carbides, nitrides, oxides, phosphides, and chalcogenides, as well as their catalytic applications. The catalytic applications mainly cover the research fields of electrocatalysis and organic catalysis. Table 4 gives the summary and quick comparison of these seven groups of metal-nonmetal nanocatalysts with their main corresponding synthesis and catalytic applications. According to these reported catalysts, researcher can choose feasible approach for the preparation of metal-nonmetal nanocrystals for specific practical applications. In addition, it was found that many well-defined metal-nonmetal nanocrystals displayed inherent advantages of high catalytic activity, selectivity, superior durability, and economic efficiency for catalytic applications. Even though considerable progress has been made in the field of metal-nonmetal nanocrystals, there are still several challenges for the development of highly efficient and stable metal-nonmetal based catalysts. Here is a shortlist of those challenges, together with the potential solutions.

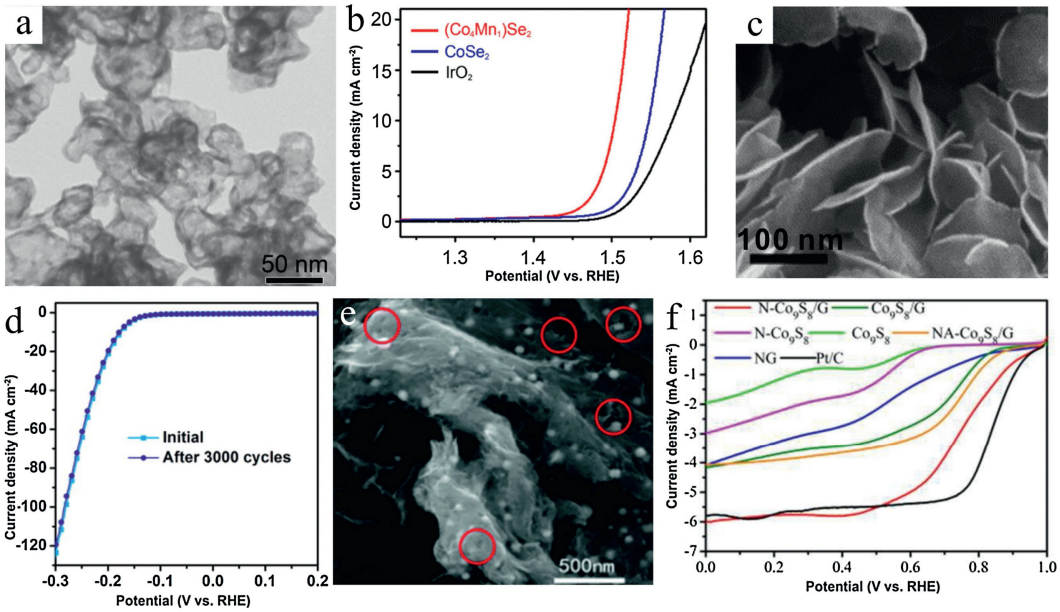

Fig. 7. (a) TEM image of ultrathin $(Co_4Mn_1)Se_2$ nanosheets and (b) the comparison of OER polarization curves of $(Co_4Mn_1)Se_2$, $CoSe_2$ and IrO_2 electrocatalysts. Reprint with permission [169]. Copyright 2018, Elsevier. (c) FE-SEM image of the typical O-MoS_2 NSs and (d) their HER polarization curves before and after 30,000 cycles. Reprint with permission [60]. Copyright 2013, American Chemical Society. (e) TEM image of N-Co_9S_8/G catalyst, the red open circles show nanosized holes induced by the NH_3-plasma etching. (f) LSV curves of the indicated electrocatalysts for ORR in O_2-saturated 0.1 mol/L KOH. Reprint with permission [58]. Copyright 2016, Royal Society of Chemistry.

(1) Precise control over the composition, size, and morphology of metal-nonmetal catalysts. Unlike introducing secondary metallic atoms into metal nanocrystals which can be routinely regarded as a common strategy now, the colloidal synthesis of high-quality metal-nonmetal nanocrystals has met with limited success, especially for noble-metal-nonmetal nanocrystals. For example, how to accurately choose the nonmetal source, metal precursor and synthetic conditions to control the morphology, particle size and composition of the products remains an unsolved problem. Generally, these parameters will change the electronic structure and chemical state of the obtained metal-nonmetal catalysts, which can affect the adsorption/desorption properties of reactant molecules or intermediates, and thus influence their catalytic behaviors. Therefore, the development of synthetic approaches, which can accurately control the composition, size and morphology of metal-nonmetal nanocrystals, are highly required and will benefit for their practical applications.

(2) Elucidating the role of nonmetallic elements in improving the catalytic performance of metal-nonmetal catalysts. Although more and more metal-nonmetal catalysts have been reported to show much enhanced catalytic performance compared with their parent metal catalysts, there are still few in-depth mechanistic studies on the role of nonmetallic elements in enhancing the catalytic activity, selectivity, and/or stability. Therefore, more attention is suggested to be paid to the mechanistic study of metal-nonmetal nanocrystals in catalytic processes. For example, the *in-situ* characterization of nonmetallic atoms and theoretical calculations of the catalytic process can help reveal the role of nonmetallic elements on the performance enhancement of metal-nonmetal catalysts, which will in turn guide the rational design of metal-nonmetal catalysts to achieve further development of catalytic performance.

In conclusion, metal-nonmetal catalysts have received considerable interest owing to their unique catalytic properties. Among them, metal hydrides, metal borides, metal carbides, metal nitrides, metal oxides, metal phosphides, and metal chalcogenides consisting of different nonmetallic elements and with tunable stoichiometries would be the most excellent candidates for catalytic applications. However, there are still many challenges that should be addressed before they can be applied in practical catalytic applications. It is hoped that the introduction of metal-nonmetal catalysts in this review can provide guidance or serve as a resource for researchers who are interested in this topic. It is

Table 4
The main preparation methods and typical catalytic applications of different metal-nonmetal nanocrystals.

Metal-nonmetal nanocrystal	Synthesis	Typical catalytic application
Metal hydrides	Gas-solid method: LiH, NaH, MgH_2, CaH_2, AlH_3, TiH_2, Sr_2MgH_6, K_2PtHH_6;	MOR: $PdH_{0.43}$; FAOR: PdH_x; ORR: $PdH_{0.706}$@Ni-B;
	Solution method: ZnH_2, K_2ReH_9, PdH_x, Ni-$PdH_{0.43}$, $PdH_{0.706}$@Ni-B;	Benzylalcohol oxidation: Ni-$PdH_{0.43}$; HOR: Ni-H; CO_2 hydrogenation: $ZrCoH_x$;
	Ion-implantation: $BaReH_9$, $LaNi_5H_6$, Mg_2H_2;	Crack ammonia: LiH, NaH, KH, MgH_2, CaH_2;
	Electrochemical synthesis: CrH	Hydrogenation/dehydrogenation: $LaNi_5$, $CaNi_5$, $LaNi_4Al$.
Metal borides	Solid-state reaction: Ni-B, Co-B, Mo-B, FeB_2, TiB_2, VB_2, $CoNiB_x$;	HER: CoB, Co_2B, MoB, MoB_2, Mo_2B, Mo_2B_4, Ni-B_x;
	Pyrolysis of metal precursor: PdB, CoB, FeB, VB_2, NbB, NbB_2, MoB, WB, TaB_2	OER: FeB, Co_2B, $CoNiB_x$; Water splitting: FeB_2, NiB_x, $CoNiB_x$, Co_2B; ORR: Pd-B; Hydrogen production: Pd-B HDS: Ni-B, Co-B; HDO: NI-Mo-B, Co-Mo-B; Syngas synthesis: Ni-B; Fischer-Tropsch reaction: Co-B; Semihydrogenation: Pd-B
Metal carbides	TPR (gas-solid reaction): Mo_2C, Fe_3C, WC, TiC, NiC, Co_3C, Cr_3C_3; MOFs-assisted method: MoC_x; Pyrolysis of metal precursors: Mo_2C, TiC, WC; Hydrothermal (solvothermal) synthesis: PdC_x	HER: TiC, Mo_2C, NiC, Co_3C, MoC, WC, Cr_7C_3; ORR: WC, Fe_3C; Water splitting: Mo_2C; Methane reforming: Mo_2C, WC; CO/H_2 oxidation: WC, ZrC, VC, Mo_2C, Cr_3C_3; HDS: Mo_2C; NH_3 decomposition: Mo_2C; Semihydrogenation: PdC_x
Metal nitrides	TPR: MoN_x, FeN_x, Ni_3N, NiMoN, W_2N, TiN, VN, Ni_3FeN, TiN@Ni_3N;	HER: W_2N, $NiMoN_x$, Ta_3N_5, MoN, Mo_2N; OER: Fe_3N, Fe_4N, Fe_xN, Ni_3N; Water splitting: Ni_3FeN, TiN@Ni_3N CO_2RR: GaN;
	Pyrolysis of metal precursors: Cu_3N, Cu_3PdN, $NiMoN_x$;	ORR: Cu_3N, Fe-N, TiN, Cu_3PdN, PdN_x; CO_2 hydrogenation: Co_4N;
	Hydrothermal (solvothermal) synthesis: TiN, FeN, WN, Mo_2N, Ni_3FeN_x, PdN_x.	FAOR: PdN_x; MOR: PdN_x; Hydroazidation: AgN_3; HDN: Mo-N; Hydroazidation of terminal alkynes: AgN_3
Metal oxides	Calcination commercial precursors: Mn-, Zn-, La-Ce-, V-, Mo-, W-oxide;	OER: RuO_2, IrO_2, CoO, CoO_x, Co_3O_4, MnO_x, $Ni_xCo_{3-x}O_4$, $ZnCo_2O_4$, $Ni_{0.9}Fe_{0.1}O_x$, $MnFe_2O_4$, $CaFeO_3$, $LaFeO_3$; HER: NiO-Ni, NiO_x;
	Precipitation method: SiO_2, Al_2O_3, TiO_2, CeO_2, V-Mo oxide, Cu-Cr oxides, V-Mo oxides; Sol-gel: NiO, V_2O_5, Nb_2O_5, Cr_2O_3, SnO_2;	Water splitting: MoO_2, $NiCo_2O_4$, CoMnO@CN; ORR: MnO_x; Acid-catalyzed reactions: SiO_2-Al_2O_3; Fisher-Tropsh reaction: Fe_2O_3;
	Vapor transport method: WO_3; Spray pyrolysis: ZnO; Thermal evaporation: V_2O_5	Fuel production: V-oxides; Biomass conversion: ZnO-Al_2O_3; Gas-phase partial oxidation of hydrocarbons: $CnMnO_2$, $CoFeO_x$; Industrial catalysts: SiO_2, Al_2O_3, TiO_2, ZnO_2, ZrO_2
Metal phosphides	Solid-state method: CoP, NiP, FeP, MoP;	HER: Ni_2P, NiP_2, Ni_5P_4, FeP, CoP, Co_2P, WP, MoP, Mo_3P, Ru_2P, RuP_2, PdP_2; OER: CoP, MoP-Ni_2P; Water splitting: CoP, Ni_2P, MoP, Rh_2P;
	Gas-solid reaction: CoP, FeP, Ni_2P, Cu_3P, MoP, Mo_3P, WP;	ORR: CoP, FeP, Ni_2P, Pt_2P; NRR: PdP_2; CO_2RR: AgP_2;
	Liquid-phase synthesis: Co_2P, FeP, Ni_2P, Ni_5P_4, $Ni1_2P_5$, Pt_2P	MOR: PdNiP; HDS/HDN/HDO: Ni_2P, Fe_2P, CoP, WP, MoP
Metal chalcogenides	Solid-state method: FeS_2, CoS_2, $Co_{0.5}Fe_{0.5}S$, Co_9S_8, NiS, MoS_2, WS_2, NiSe, $CoSe_2$, $CoTe_2$, Ni_3Se_2;	HER: FeS_2, CoS_2, Co_3S_4, NiS, FeNiS, MoS_2, MoS_x, WS_2, NiSe, Ni_3Se_2, CoSe, $CoSe_2$, CoPSe, MoS_x; OER: Ni_3S_2, Fe_7S_8, Co_3S_4, $CoSe_2$, $CoTe_2$;
	Molten flux synthesis: NiS_x, CoSe, ReS_2;	Water splitting: NiS_x, MoS_2@Ni, MoS_2-Ni_3S_2; ORR: $Co_3FeS_{1.5}(OH)_6$, Co_9S_8; HDS/HDN/HDY: MoS_2, NbS_2, ReS_2, RuS_2, Co_9S_8;
	Hydro(solvo)thermal synthesis: CoS@CNT, CoS_2, Co_3S_4, Co_9S_8, NiS_2, Ni_3S_2, $CoSe_2$, NiSe	Semihydrogenation: PdS, Pd@$SPhF_2$

believed that this new class of catalysts would be the most promising candidate for noble metal catalysts, playing important role in catalysis, especially in electrocatalysis.

Declaration of competing interest

We declare that we have no financial and personal relationships with other people or organizations that can inappropriately influence our work, there is no professional or other personal interest of any nature or kind in any product, service and/or company that could be construed as influencing the position presented in, or the review of, the manuscript entitled.

Acknowledgments

M. Jin acknowledges the support of the National Natural Science Foundation of China (NSFC, Nos. 21773180 and 21471123), State Key Laboratory for Mechanical Behavior of Materials, "the Fundamental Research Funds for the Central Universities" and "the World-Class Universities (Disciplines) and the Characteristic Development Guidance Funds for the Central Universities" by Xi'an Jiaotong University.

References

[1] R.C. Baetzold, R.E. Mack, J. Chem. Phys. 62 (1975) 1513–1520.
[2] V.I. Klimov, Semiconductor and Metal Nanocrystals: Synthesis and Electronic and Optical Properties, 1st ed., CRC Press, Florida, 2003.
[3] Y. Hou, S. Gao, J. Alloys Compd. 365 (2004) 112–116.
[4] A. Nag, D.S. Chung, D.S. Dolzhnikov, et al., J. Am. Chem. Soc. 134 (2012) 13604–13615.
[5] H. Jahangirl, J. Bennett, P. Mahjoubi, K. Wilson, S. Gu, Catal. Sci. Technol. 4 (2014) 2210–2229.
[6] M.K. Samantaray, R. Dey, S. Kavitake, et al., J. Am. Chem. Soc. 138 (2016) 8595–8602.
[7] W. Wang, X. Li, T. He, Y. Liu, M. Jin, Nano Lett. 19 (2019) 1743–1748.
[8] X. Li, Z. Wang, Z. Zhang, et al., Mater. Horiz. 4 (2017) 584.
[9] A.A. Peterson, J.K. Nørskov, J. Phys. Chem. Lett. 3 (2012) 251–258.
[10] P. Yu, M. Pemberton, P. Plasse, J. Power Sources 144 (2005) 11–20.
[11] M. Pourbaix, Altas of Electrochemical Equilibrium in Aqueous Solutions, 2nd ed., Pergamon Press, New York, 1966.
[12] Y. Liu, C. Wang, W. Wang, et al., Nanoscale 11 (2019) 14828.
[13] M. Ahmadi, H. Mistry, B.R. Cuenya, J. Phys. Chem. Lett. 7 (2016) 3519–3533.
[14] J.R. Norton, J. Sowa, Chem. Rev. 116 (2016) 8315–8317.
[15] S. Kato, S.K. Matam, P. Kerger, et al., Angew. Chem. Int. Ed. 128 (2016) 6132–6136.
[16] T. Zhang, H. Miyaoka, H. Miyaoka, T. Ichikawa, Y. Kojima, ACS Appl. Energy Mater. 1 (2018) 232–242.
[17] M.M.H. Bhuiya, A. Kumar, K.J. Kim, Int. J. Hydrogen Energy 40 (2015) 2231–2247.
[18] Z. Zhao, X. Huang, M. Li, et al., J. Am. Chem. Soc. 137 (2015) 15672-1567.
[19] C. Zhan, H. Li, X. Li, Y. Jiang, Z. Xie, Sci. China Mater. 63 (2020) 375–382.
[20] J. Zhang, M. Chan, H. Li, et al., Nano Energy 44 (2018) 127–134.
[21] Y. Lu, J. Wang, Y. Peng, A. Fisher, X. Wang, Adv. Energy Mater. 7 (2017) 1700919.
[22] H. Li, P. Wen, Q. Li, et al., Adv. Energy Mater. 7 (2017) 1700513.
[23] J. Masa, P. Weide, D. Peeters, et al., Adv. Energy Mater. 6 (2016) 1502313.
[24] S.E. Skrabalak, K.S. Suslick, Chem. Mater. 18 (2006) 3103–3107.
[25] L. Chen, Y. Lu, Q. Hong, J. Lin, F.M. Dautzenberg, Appl. Catal. A: Gen. 292 (2005) 295–304.
[26] R. Ma, Y. Zhou, Y. Chen, et al., Angew. Chem. Int. Ed. 54 (2015) 14723–14727.
[27] K. Zhang, Y. Zhao, D. Fu, Y. Chen, J. Mater. Chem. A 3 (2015) 5783–5788.
[28] X. Fan, H. Zhou, X. Guo, ACS Nano 9 (2015) 5125–5134.
[29] A.L. Stottlemyer, E.C. Weigert, J.G. Chen, Ind. Eng. Chem. Res. 50 (2011) 16–22.
[30] N.I. Il'Chenko, Y.I. Pyatnitskii, N.V. Pavlenko, Theor. Exp. Chem. 34 (1998) 239–256.
[31] A.J. Brungs, A.P. York, M.L. Green, Catal. Lett. 57 (1999) 65–69.
[32] W. Zheng, T.P. Cotter, P. Kaghazchi, et al., J. Am. Chem. Soc. 135 (2013) 3458–3464.
[33] R. Guo, Q. Chen, X. Li, et al., J. Mater. Chem. A 7 (2019) 4714–4720.
[34] J.G. Choi, J.R. Brenner, C.W. Colling, et al., Catal. Today 15 (1992) 201–222.
[35] J.C. Schlatter, S.T. Oyama, J.E. Metcalfe III, et al., Ind. Eng. Chem. Res. 27 (1998) 1648–1653.
[36] H. Wu, W. Chen, J. Am. Chem. Soc. 133 (2011) 15236–15239.
[37] K. Xu, P. Chen, X. Li, et al., J. Am. Chem. Soc. 137 (2015) 4119–4125.
[38] W.F. Chen, K. Sasaki, C. Ma, et al., Angew. Chem. Int. Ed. 51 (2012) 6131–6135.
[39] F. Yu, H. Zhou, Z. Zhu, et al., ACS Catal. 7 (2017) 2052–2057.
[40] R. Guo, K. Zhang, Y. Liu, et al., J. Mater. Chem. A 9 (2021) 6196–6204.
[41] J. Védrine, Catalysts 7 (2017) 341.
[42] A.P.S. Chouhan, A.K. Sarma, Renew. Sust. Energ. Rev. 15 (2011) 4378–4399.
[43] J.L. Callahan, R.K. Grasselli, J. AlChE 9 (1963) 755–760.
[44] Y. Jin, H. Wang, J. Li, et al., Adv. Mater. 28 (2016) 3785–3790.
[45] Y. Jin, P.K. Shen, J. Mater. Chem. A 3 (2015) 20080–20085.
[46] L. Yang, J. Yu, Z. Wei, et al., Nano Energy 41 (2017) 772–779.
[47] W.T. Hong, M. Risch, K.A. Stoerzinger, et al., Energy Environ. Sci. 8 (2015) 1404–1427.
[48] J. Pan, X.L. Tian, S. Zaman, et al., Batter. Supercaps 2 (2018) 336–347.
[49] A.B. Laursen, K.R. Patraju, M.J. Whitaker, et al., Energy Environ. Sci. 8 (2015) 1027–1034.
[50] S.T. Oyama, T. Gott, H. Zhao, Y.L. Lee, Catal. Today 143 (2009) 94–107.
[51] J.F. Callejas, C.G. Read, E.J. Popczun, J.M. McEnaney, R.E. Schaak, Chem. Mater. 27 (2015) 3769–3774.
[52] Z. Pu, Q. Liu, A.M. Asiri, X. Sun, ACS Appl. Mater. Interfaces 6 (2014) 21874–21879.
[53] J. Tian, Q. Liu, N. Cheng, A.M. Asiri, X. Sun, Angew. Chem. Int. Ed. 53 (2014) 9577–9581.
[54] T. Liu, L. Xie, J. Yang, et al., ChemElectroChem 4 (2017) 1840–1845.
[55] C. Du, M. Shang, J. Mao, W. Song, J. Mater. Chem. A 5 (2017) 15940–15949.
[56] C.P. Lee, W.F. Chen, T. Billo, et al., J. Mater. Chem. A 4 (2016) 4553–4561.
[57] B. Hinnemann, P.G. Moses, J. Bonde, et al., J. Am. Chem. Soc. 127 (2005) 5308–5309.
[58] S. Dou, L. Tao, J. Huo, S. Wang, L. Dai, Energy Environ. Sci. 9 (2016) 1320–1326.
[59] Y. Qi, L. Zhang, L. Sun, et al., Nanoscale 12 (2020) 1985–1993.
[60] J. Xie, J. Zhang, S. Li, et al., J. Am. Chem. Soc. 135 (2013) 17881–17888.
[61] H. Kohlmann, Metal Hydrides, Encyclopedia of Physical Science and Technology, 3rd ed., Academic Press, 2003.
[62] K. Young, Metal Hydrides, BASF/Battery Materials-Ovonic, 1st ed., Elsevier, Michigan, 2013.
[63] N. Nishimiya, K. Numata, H. Saito, T. Mori, S. Miyake, Hydrogen Absorbing Films Prepared by Ion Beam Assisted Deposition, 1st ed., Novel Materials Processing, 2005.
[64] S. Suda, G.S. Zeit, Phys. Chem. 183 (1994) 149.
[65] F. Schüth, B. Bogdanović, M. Felderhoff, Chem. Commun. 5 (2004) 2249–2258.
[66] B. Sakintuna, F. Lamari-Darkrim, Int. J. Hydrogen Energy 32 (2007) 1121–1140.
[67] J.W. Sheffield, K.B. Martin, Electricity and Hydrogen as Energy Vectors for Transportation Vehicles, Woodhead Publishing, 2014.
[68] S. Gupta, N. Patel, A. Miotello, D.C. Kothari, J. Power Sources 279 (2015) 620–625.
[69] P. Zhang, M. Wang, Y. Yang, et al., Nano Energy 19 (2016) 98–107.
[70] H. Vrubel, X. Hu, Angew. Chem. Int. Ed. 51 (2012) 12703–12706.
[71] G. Akopov, I. Roh, Z.C. Sobell, et al., J. Am. Chem. Soc. 139 (2017) 17120–17127.
[72] P.R. Jothi, K. Yubuta, B.P.T. Fokwa, Adv. Mater. 30 (2018) e1704181.
[73] H. Park, A. Encinas, J.P. Scheifers, Y. Zhang, B.P.T. Fokwa, Angew. Chem. Int. Ed. 56 (2017) 5575–5578.
[74] B.P.T. Fokwa, P.R.N. Misse, M. Gilleßen, R. Dronskowski, J. Alloy Compd. 489 (2010) 339–342.
[75] H. Park, Y. Zhang, J.P. Scheifers, et al., J. Am. Chem. Soc. 139 (2017) 12915–12918.
[76] N. Patel, R. Fernandes, G. Guella, et al., J. Phys. Chem. C 112 (2008) 6968–6976.
[77] N. Xu, G. Cao, Z. Chen, et al., J. Mater. Chem. A 5 (2017) 12379–12384.
[78] J. Xu, L. Chen, K. Tan, A. Borgna, M. Saeys, J. Catal. 261 (2009) 158–165.
[79] K.F. Tan, J. Chang, A. Borgna, M. Saeys, J. Catal. 280 (2011) 50–59.
[80] W. Wang, Y. Yang, J. Bao, H. Luo, Catal. Commun. 11 (2009) 100–105.
[81] W. Wang, Y. Yang, H. Luo, T. Hu, W. Liu, Catal. Commun. 12 (2011) 436–440.
[82] K. Jiang, K. Xu, S. Zou, W.B. Cai, J. Am. Chem. Soc. 136 (2014) 4861–4864.
[83] C.W. Chan, A.H. Mahadi, M.M. Li, et al., Nat. Commun. 5 (2014) 5787.
[84] B. Jiang, X.G. Zhang, K. Jiang, D.Y. Wu, W.B. Cai, J. Am. Chem. Soc. 140 (2018) 2880–2889.
[85] L.E. Toth, Transition Metal Carbides and Nitrides, 1st ed., Academic Press, New York and London, 1971.
[86] L. Liao, S. Wang, J. Xiao, et al., Energy Environ. Sci. 7 (2014) 387–392.
[87] F.X. Ma, H.B. Wu, B.Y. Xia, C.Y. Xu, X.W. Lou, Angew. Chem. Int. Ed. 54 (2015) 15395–15399.
[88] H.B. Wu, B.Y. Xia, L. Yu, X.Y. Yu, X.W. Lou, Nat. Commun. 6 (2015) 6512.
[89] D.V. Esposito, J. Chen, Energy Environ. Sci. 4 (2011) 3900.
[90] R.B. Levy, M. Boudart, Science 181(4099) 547-549.
[91] S.T. Oyama, Catal. Today 15 (1992) 179–200.
[92] R. Michalsky, Y.J. Zhang, A.A. Peterson, ACS Catal. 4 (2014) 1274–1278.
[93] M.C. Weidman, D.V. Esposito, Y.C. Hsu, J.G. Chen, J. Power Sources 202 (2012) 11–17.
[94] M. Xiao, J. Zhu, L. Feng, C. Liu, W. Xing, Adv. Mater. 27 (2015) 2521–2527.
[95] M.S. Balogun, Y. Huang, W. Qiu, et al., Mater. Today 8 (2017) 425–451.
[96] L. Wang, W. Zhang, X. Zheng, et al., Nat. Energy 2 (2017) 869–876.
[97] L. Volpe, M. Boudart, J. Solid State Chem. 59 (1985) 332–347.
[98] X. Ren, G. Cui, L. Chen, et al., Chem. Commun. 54 (2018) 8474–8477.
[99] E.G. Gillan, B.R. Kaner, Inorg. Chem. 33 (1994) 5693e5700.
[100] B. Avasarala, T. Murray, W. Li, P. Haldar, J. Mater. Chem. 19 (2009) 1803.
[101] M.M.O. Thotiyl, S. Sampath, Electrochim. Acta 56 (2011) 3549–3554.
[102] F. Liu, X. Yang, D. Dang, X. Tian, ChemElectroChem 6 (2019) 2208–2214.
[103] H. Nan, D. Dang, X.L. Tian, J. Mater. Chem. A 6 (2018) 6065–6073.
[104] K. Ojha, S. Saha, B. Kumar, K.S. Hazra, A.K. Ganguli, ChemCatChem 8 (2016) 1218–1225.

[105] W.-J. Jiang, L. Gu, L. Li, et al., J. Am. Chem. Soc. 138 (2016) 3570–3578.
[106] S. Cao, Q. Ji, H. Li, et al., J. Am. Chem. Soc. 142 (2020) 7083–7091.
[107] D.D. Vaughn II, J. Araujo, P. Meduri, et al., Chem. Mater. 26 (2014) 6226–6232.
[108] X. Carrier, S. Royer, E. Marceau, Synthesis of metal oxide catalysts, in: J.C. Védrine (Ed.), Metal Oxides in Heterogeneous Catalysis, Elsevier, 2018, pp. 43–103.
[109] D. Zappa, A. Bertuna, E. Comini, et al., Beilstein J. Nanotechnol. 8 (2017) 1205–1217.
[110] J.C. Védrine, Catalysts 7 (2017) 341.
[111] B. Pawelec, Surface processes and composition of metal oxide surfaces, in: J.L. G. Fierro (Ed.), Metal Oxides, Chemistry and Applications, CRC Press, Florida, 2006, pp. 111–193.
[112] R.J. Davis, Z. Liu, Chem. Mater. 9 (1997) 2311–2324.
[113] E. Loni, M.H. Siadati, A. Shokuhfar, Mater. Today Energy 16 (2020) 100398.
[114] F. Song, X. Hu, Nat. Commun. 5 (2014) 4477.
[115] H. Jin, J. Wang, D. Su, et al., J. Am. Chem. Soc. 137 (2015) 2688–2694.
[116] Y. Wang, T. Zhou, K. Jiang, et al., Adv. Energy Mater. 4 (2014) 1400696.
[117] R. Jiang, D.T. Tran, J. Li, D. Chu, Energy Environ. Mater. 2 (2019) 201–208.
[118] Si. Chen, H. Huang, P. Jiang, et al., ACS Catal. 10 (2020) 1152–1160.
[119] K. Fominykh, P. Chernev, I. Zaharieva, et al., ACS Nano 9 (2015) 5180–5188.
[120] Z.Q. Liu, H. Cheng, N. Li, T.Y. Ma, Y.Z. Su, Adv. Mater. 28 (2016) 3777–3784.
[121] G. Gardner, J. Al-Sharab, N. Danilovic, et al., Energy Environ. Sci. 9 (2016) 184–192.
[122] Y. Tong, P. Chen, T. Zhou, et al., Angew. Chem. Int. Ed. 56 (2017) 7121–7125.
[123] M. Sun, H. Liu, J. Qu, et al., Adv. Energy Mater. 6 (2016) 1600087.
[124] J.F. Callejas, C.G. Read, C.W. Roske, N.S. Lewis, R.E. Schaak, Chem. Mater. 28 (2016) 6017–6044.
[125] R. Prins, M.E. Bussell, Catal. Lett. 142 (2012) 1413–1436.
[126] Y. Shi, B. Zhang, Chem. Soc. Rev. 45 (2016) 1529–1541.
[127] H. Wu, Y. Cheng, B. Wang, et al., J. Energy Chem. 57 (2021) 198–205.
[128] R. Guo, W. Bi, K. Zhang, et al., Chem. Mater. 31 (2019) 8205–8211.
[129] A.E. Henkes, Y. Vasquez, R.E. Schaak, J. Am. Chem. Soc. 129 (2007) 1896–1897.
[130] H. Tianou, W. Wang, X. Yang, et al., Nat. Commun. 8 (2017) 1261.
[131] Y. Bai, H. Zhang, L. Fang, et al., J. Mater. Chem. A 3 (2015) 5434–5441.
[132] S.J. Sawhill, D.C. Phillips, M.E. Bussell, J. Catal. 215 (2003) 208–219.
[133] Y. Pan, Y. Liu, J. Zhao, et al., J. Mater. Chem. A 3 (2015) 1656–1665.
[134] F.H. Saadi, A.I. Carim, E. Verlage, et al., J. Phys. Chem. C 118 (2014) 29294–29300.
[135] J. Tian, Q. Liu, A.M. Asiri, X. Sun, J. Am. Chem. Soc. 136 (2014) 7587–7590.
[136] H. Wu, Y. Cheng, B. Wang, et al., J. Energy Chem. 57 (2021) 198–205.
[137] V. Zuzaniuk, R. Prins, J. Catal. 219 (2003) 85–96.
[138] Y. Liang, Q. Liu, A.M. Asiri, et al., ACS Catal. 4 (2014) 4065–4069.
[139] S. Han, Y. Feng, F. Zhang, et al., Adv. Funct. Mater. 25 (2015) 3899–3906.
[140] H. Song, Y. Li, L. Shang, et al., Nano Energy 72 (2020) 104730.
[141] H. Li, P. Wen, D.S. Itanze, et al., Nat. Commun. 10 (2019) 5724.
[142] P. Liu, J.A. Rodriguez, J. Am. Chem. Soc. 127 (2005) 14871–14878.
[143] P. Xiao, M.A. Sk, L. Thia, et al., Energy Environ. Sci. 7 (2014) 2624.
[144] P.E. Blanchard, A.P. Grosvenor, R.G. Cavell, Chem. Mater. 20 (2008) 7081–7088.
[145] H. Xie, Q. Geng, X. Zhu, et al., J. Mater. Chem. A 7 (2019) 24760–24764.
[146] H. Song, Y. Cheng, B. Li, et al., ACS Sustainable Chem. Eng. 8 (2020) 3995–4002.
[147] Y. Zhang, Q. Zhou, J. Zhu, et al., Adv. Funct. Mater. 35 (2017) 1702317.
[148] M.G. Kanatzidis, K.R. Poeppelmeier, Prog. Solid State Chem. 36 (2008) 1–133.
[149] W. Xiong, G. Zhang, Q. Zhang, Inorg. Chem. Front. 1 (2014) 292–301.
[150] P.R. Bonneau, R.F. Jarvis, R.B. Kaner, Nature 349 (1991) 510–512.
[151] J. Zhou, J. Lin, X. Huang, et al., Nature 556 (2018) 355–359.
[152] N. Jiang, Q. Tang, M. Sheng, et al., Catal. Sci. Technol. 6 (2016) 1077–1084.
[153] B. You, N. Jiang, M. Sheng, Y. Sun, Chem. Commun. 51 (2015) 4252–4255.
[154] M. Fan, R. Gao, T. Zou, et al., Electrochim. Acta 215 (2016) 366–373.
[155] C.J. Jacobsen, E. Törnqvist, H. Topsøe, Cataly. Lett. 63 (1999) 179–183.
[156] X. Zhao, L. Zhou, W. Zhang, et al., Chem 4 (2018) 1080–1091.
[157] M.S. Faber, M.A. Lukowski, Q. Ding, N.S. Kaiser, S. Jin, Phys. Chem. C 118 (2014) 21347–21356.
[158] J. Zhu, Y. Koltypin, A. Gedanken, Chem. Mater. 12 (2000) 73–78.
[159] W. Zhu, X. Yue, W. Zhang, et al., Chem. Commun. 52 (2016) 1486–1489.
[160] X. Long, G. Li, Z. Wang, et al., J. Am. Chem. Soc. 137 (2015) 11900–11903.
[161] D.Y. Wang, M. Gong, H.L. Chou, et al., J. Am. Chem. Soc. 137 (2015) 1587–1592.
[162] J. Shi, J. Hu, Y. Luo, X. Sun, A.M. Asiri, Catal. Sci. Technol. 5 (2015) 4954–4958.
[163] M.R. Gao, J. Liang, Y. Zheng, et al., Nat. Commun. 6 (2015) 5982–5988.
[164] D. Kong, H. Wang, Z. Hu, Y. Cui, J. Am. Chem. Soc. 136 (2014) 4897–4900.
[165] C. Tang, N. Cheng, Z. Pu, W. Xing, X. Sun, Angew. Chem. Int. Ed. 54 (2015) 9351–9355.
[166] T. Liu, A.M. Asiri, X. Sun, Nanoscale 8 (2016) 3911–3915.
[167] M. Xiao, Y. Miao, Y. Tian, Y. Yan, Electrochim. Acta 165 (2015) 206–210.
[168] Y. Liu, H. Cheng, M. Lyu, et al., J. Am. Chem. Soc. 136 (2014) 15670–15675.
[169] X. Zhao, X. Li, Y. Yan, et al., Appl. Catal. B: Environ. 236 (2018) 569–575.
[170] S. Zhao, R. Jin, H. Abroshan, et al., J. Am. Chem. Soc. 139 (2017) 1077–1080.
[171] X. Zhou, H. Zhang, Y. Yan, et al., Angew. Chem. Int. Ed. 55 (2016) 1–6.
[172] R. He, J. Hua, A. Zhang, et al., Nano Lett. 17 (2017) 4311–4316.
[173] X. Zhao, Y. Xing, L. Zhao, et al., J. Catal. 368 (2018) 155–162.
[174] R. He, A. Zhang, Y. Ding, et al., Adv. Mater. 30 (2018) 1705872.
[175] N.S. Choi, Z. Chen, S.A. Freunberger, et al., Angew. Chem. Int. Ed. 51 (2012) 9994–10024.
[176] Y. Min, E. Im, G. Hwang, et al., Nano Res. 12 (2019) 1750–1769.
[177] D. Jasion, J.M. Barforoush, Q. Qiao, et al., ACS Catal. 5 (2015) 6653.
[178] X. Qian, J. Liu, L. Fu, J. Li, Science 346 (2014) 1344–1347.
[179] D. Xiao, G. Liu, W. Feng, et al., Phys. Rev. Lett. 108 (2012) 196802.
[180] Y. Saito, T. Nojima, Nat. Rev. Mater. 2 (2017) 16094.